Growth of Non-necrotic Tumours in the Presence and Absence of Inhibitors

H.M. Byrne & M.A.J. Chaplain

School of Mathematical Sciences

University of Bath

Claverton Down

Bath BA2 7AY

phone: +(44) 01225 826242

FAX: +(44) 01225 826492

e-mail: hmb,majc@maths.bath.ac.uk

running title: non-necrotic tumour growth

Abstract

In this paper a model for the evolution of a spherically symmetric, non-necrotic tumour is presented. The effects of nutrients and inhibitors on the existence and stability of time-independent solutions are studied. With a single nutrient and no inhibitors present the trivial solution, which corresponds to a state in which no tumour is present, persists for all parameter values whereas the nontrivial solution, which corresponds to a tumour of finite size, exists for only a prescribed range of parameters, corresponding to a balance between cell proliferation and cell death. Stability analysis, based on a two-timing method, suggests that, where it exists, the nontrivial solution is stable and the trivial solution unstable. Otherwise, the trivial solution is stable. Modifications to these characteristic states brought about by the presence of different types of inhibitors are also investigated and shown to have significant effect. Implications of the model for the treatment of cancer are also discussed.

Revised Version Submitted to Mathematical Biosciences December 13, 1994

1 Introduction

Over the past twenty years an increasing number of mathematical models describing solid tumour growth have appeared in the literature [1], [2], [3], [4], [5], [6], [7]. Analysis of such models enables the relative importance of the different mechanisms involved in the growth process to be examined and may also assist in assessing the relative merits of different courses of drug treatment or chemotherapy [8], [9], [10], [11], [12]. Many of the existing deterministic tumour models consist of an ordinary differential equation, coupled to one, or more, reaction-diffusion equations. The ordinary differential equation derives from mass conservation applied to the tumour and describes the evolution of the tumour boundary, whereas the reaction-diffusion equations describe the distribution, within the tissue, of nutrients, such as oxygen and glucose, and growth inhibitory factors (GIFs), such as chalones.

In this paper, the evolution of a single tumour, prior to the onset of necrosis, is discussed, with particular attention focussed on the existence, and stability, of steady-state tumour configurations, in which there is a balance between cell proliferation and cell death or apoptosis. Modifications to the tumour's growth characteristics induced by the presence of an inhibitor are analysed, with a view to assessing the efficacy of certain cancer treatments. For simplicity of exposition, a single nutrient species and single inhibitor species are considered, so that the model comprises two coupled reaction-diffusion equations for each species and an integro-differential equation, which describes the evolution of the tumour boundary.

The inclusion of phenomena such as diffusion and nutrient consumption renders the model similar to those of, for example, Adam, Greenspan and Maggelakis [1], [2], [5], [6], [7]. However, a number of features distinguishes this work from theirs. The latter models have particular relevance to in vitro situations where multicell spheroids are grown in isolation in petri dishes and diffusion is the only transport mechanism for externally supplied nutrients and inhibitors [13], [9]. This situation is not necessarily the case in vivo. For example, an avascular tumour with a proximal host vasculature may become vascularised before a necrotic core has developed, as a result of the emission of tumour angiogenesis factor (TAF) [14], [15]. The chemoattractant TAF stimulates neighbouring capillaries to form sprouts which, in turn, migrate towards the tumour, furnishing it with its own blood supply, in order that cells may receive nourishment not only via diffusion but also by blood-tissue transfer. If we assume that the blood-tissue exchange rate is proportional to the difference in nutrient concentration between the tumour/tissue (σ) and the vasculature (σ_B), then the model presented applies to the subsequent growth of the vascular tumour. Alternatively, by reinterpreting the nutrient source and sink terms (setting $\Gamma = 0$), our model may also describe the avascular phase of tumour growth.

The fact that the majority of existing models focus on in vitro growth of multicell spheroids has limited the inhibitory mechanisms considered to those induced by the tumour itself. For example, Adam and Maggelakis examine the effect on tumour development of a growth inhibitory factor secreted by its necrotic core. The tumour configuration postulated in this paper leads naturally to a discussion of a wider range of inhibitory behaviour. For example, the efficacy of an anti-cancer drug delivered to the tumour by the host vasculature can be compared with a therapy designed to administer the drug by diffusion from neighbouring tissue. In addition, the action of naturally-occurring inhibitors, stimulated by the immune system in healthy cells, in response to the foreign body, can be assessed. As the analysis shows, this natural regulatory mechanism provides a possible explanation for the dormant tumours observed in healthy animals [13], [15], [16]. It also provides an explanation for malignancies which disappear: it is widely believed that undetected malignancies which disappear naturally are a common feature in animals such as man [16].

The second difference between this work and that of, for example, [1], [6], [7] is the inclusion of a natural cell loss mechanism, 'apoptosis' or 'shrinkage necrosis', in the mass conservation equation, governing the evolution of the tumour radius (see [17], [18], [12] for a description of the structural changes involved in apoptosis). Motivation for the inclusion of such a term stems from the existence of dormant tumour states [12]. Greenspan modelled this cell loss as a pressure gradient driven migration of cells from the tumour's outer rim to the necrotic core where they disintegrate into highly permeable waste products [6]. However, Durand's observations [19] of only a small proportion of labelled nuclei in the necrotic core of a spheroid labelled with tritiated thymidine, a marker of DNA, strongly suggest that other cell loss mechanisms may occur. Other experiments support this view. Sutherland and Durand [11] observed no increase in the size of non-necrotic multicell spheroids undergoing starvation. Further, Kerr *et al.* [17], [18] found that apoptosis can always be detected in neoplasms. In conclusion, it is highly likely that apoptosis is the cause of the observed volume loss in solid spheroids in vivo and should, therefore, be included in any mathematical model describing their evolution. To date, only McElwain and Morris [20] have incorporated apoptosis into a mathematical model, by assuming a constant cell (or, equivalently, nutrient) loss rate in mitosing regions. Under certain conditions, their model admits *dormant* states which do not possess necrotic cores. The dormant states possess a two-layer structure: an outer, proliferating rim, enveloping a layer in which the rates of nutrient consumption and cell proliferation fall. By contrast, the model proposed in this paper admits mono-layer dormant solutions, which correspond to a tumour comprising only viable, proliferating cells, in which the flux and consumption of nutrient are in equilibrium. In section 4 we show that this feature is crucial to the existence of nontrivial steady configurations, for which the central necrotic core is absent. Without this cell-loss term, no such solutions exist and the familiar results of [1], [2], [5], [6], [7] are recovered, with exponential growth of the tumour throughout phase I predicted. (Here, a phase I tumour is defined to be a tumour comprising only active proliferating cells with no regions of necrosis evident.)

A further feature of this work arises from the two timescales intrinsic to tumour growth [1], [2]: the first related to the growth rate of the tissue and the second related to nutrient diffusion. Given that a fast-growing tumour may expand at a rate of up to 0.5 mm/day and that a typical diffusion time scale is 1 min ($\equiv L^2/D$, where $L \sim 10^{-2}$ cm is a typical length scale and $D \sim 10^{-6}$ cm^2 s^{-1} a typical diffusion coefficient), it is clear that the diffusion timescale of nutrients and inhibitors is much shorter than the growth timescale. Existing work [1], [2], [6], [20] exploits this difference, to simplify the analysis, by neglecting the diffusion timescale and focussing on the longer, tumour growth timescale, through the adoption of a quasi-steady approach, with $\partial/\partial t \equiv 0$ in any reaction-diffusion equations. Stability is then interpreted as meaning attainment of a quasi-steady configuration. Here, however, variation of the dependent variables on both timescales is permitted and the problem may be recast in a form suitable for two-timing analysis [21], [22]. This distinction enables us to gain insight into the previously unstudied, transient behaviour of tumours, without affecting either the longer timescale dynamics or the nature of the steady solutions since, by definition, these possess no temporal dependence. Stability of the resulting steady solutions is assessed by examining the longer-time behaviour of the system, a stable configuration, if it exists, being attained in this limit. The result of adopting this approach is that, for certain parameter regimes, and, in particular, when no inhibitor is present, stability of the (trivial) steady phase I solution is predicted. Further, when instability of the trivial solution is predicted it is possible to identify key parameters which, when altered, will allow the system to approach the trivial stable configuration. For example, increasing the cell death rate ($\tilde{\sigma}$) or decreasing the external nutrient concentration (σ_R) stabilises the trivial solution.

The outline of the paper is as follows. The model of tumour growth being studied is presented in section 2. Following Chaplain and Britton [23], and to simplify the analysis, attention is restricted to a spherically symmetric tumour. The model is time-dependent with the outer radius of the tumour, denoted by $R(t)$, nonlinearly dependent on the nutrient and inhibitor concentrations within the tumour. Numerical solutions of the resulting dimensionless model are presented in section 3 whilst in section 4 steady, time-independent solutions of the model are constructed. A bound constraining the system's parameters is derived as a necessary condition for the existence of such steady solutions in the absence of any inhibitor. In physical terms, there should be a balance between the net flux and consumption rates of nutrient in the tumour. Modifications to these steady-states brought about by the presence of an inhibitor are then investigated. In particular, cases for which the steady-state is smaller (larger) as a result of the inhibitor are presented, and the appearance of a second nontrivial steady-state observed for certain parameter values. The stability of these solutions is addressed in section 5 using the method of multiple scales. For the inhibitor-free model, where it exists, the nontrivial solution is shown to be stable and the trivial solution unstable. Conversely, where no nontrivial solutions exist the trivial solution is stable. The affect that the inhibitor species induces on the stability of these steady solutions is also considered. For example, we show how, by increasing the externally prescribed inhibitor concentration, the trivial steady-state may be rendered stable. These analytical results are borne out by the numerical simulations of section 3. Section 6 concludes with a brief summary of the results, together with a discussion of their implications for the treatment of cancer patients.

2 Model Equations

A brief description of the tumour-growth model which we study is presented below (fuller derivations can be found in [1], [2], [5], [6], [7]). Treating the tumour as a growing spherical mass, with radial symmetry, we employ a one-space-dimensional model to describe the tumour's evolution. This assumption simplifies the mathematical analysis. The model comprises two reaction-diffusion equations, which describe the distribution of externally supplied nutrient and inhibitor species, and an integro-differential equation, which governs the evolution of the tumour's outer radius.

Consider a spherically symmetric tumour, of radius $R(t)$. If, as mentioned in the introduction, the tumour possesses its own vasculature then nutrient, essential to the survival of the tumour, may be supplied via the capillary network at a rate $\Gamma(\sigma - \sigma_B)$, where σ is the nutrient concentration in the tumour (or tissue), σ_B is the constant nutrient concentration in the vasculature, and Γ is the rate of blood-tissue transfer per unit length, also assumed constant. Thus, whenever there is an imbalance in the nutrient concentration between the tumour and its vasculature, this transfer mechanism acts to redress it, and for the avascular case we have $\Gamma = 0$. Nutrient diffuses throughout the tumour, with (assumed constant) diffusion coefficient D_1, and, in the absence of inhibitor, is consumed at the rate $\lambda\sigma$. The presence in the tumour of inhibitor (β) acts as a second sink of nutrient at rate $g_1(\sigma, \beta)$, which we discuss below. Denoting by r, t the spatial and temporal independent variables, the resulting, one-dimensional, reaction-diffusion equation is given by:

$$\frac{\partial \sigma}{\partial t} = \frac{D_1}{r^2}\frac{\partial}{\partial r}\left(r^2 \frac{\partial \sigma}{\partial r}\right) + \Gamma(\sigma_B - \sigma) - \lambda\sigma - g_1(\sigma, \beta). \tag{1}$$

As mentioned above, the inclusion in equation (1) of a term describing blood-tissue transfer distinguishes this model from existing models. For more realistic descriptions of heterogeneous vascular tumours, perhaps possessing necrotic cores, a spatially-varying transfer coefficient $\Gamma = \Gamma(r)$ should be employed – indeed, future work will address this modification. In practice, expressions for vascular exchange, together with nutrient consumption, may be obtained from experimental measurements: we choose to employ simplistic reaction terms in order to demonstrate the analytical techniques as clearly as possible.

Assuming that similar effects govern the evolution of the inhibitor in the tumour, the following reaction-diffusion equation is also obtained:

$$\frac{\partial \beta}{\partial t} = \frac{D_2}{r^2}\frac{\partial}{\partial r}\left(r^2 \frac{\partial \beta}{\partial r}\right) - g_2(\sigma, \beta), \tag{2}$$

where D_2 is the inhibitor diffusion concentration, and, for simplicity, all sinks and sources of inhibitor are now combined in the single term $g_2(\sigma, \beta)$, discussed below. For example, for a blood-borne anti-cancer drug, a blood-tissue exchange rate of the form $\Gamma(\beta - \beta_B)$ should be incorporated into $g_2(\sigma, \beta)$. Conversely, for inhibitors secreted by neighbouring healthy cells, in response to the 'foreign' body, no such term is necessary; the inhibitor is delivered by diffusion across the tumour boundary.

The rate of growth of the tumour is dependent on the number of proliferating cells contained inside it. Assuming that this active cell density is, in turn, a function of the nutrient and inhibitor concentrations, no explicit mention need be made of the cell density henceforth, an appropriate function of σ and β replacing it [6], [20]. (Future work will address the importance of making this simplifying assumption.) Denoting by $S(\sigma, \beta)$ the cell proliferation rate at a point inside the tumour, mass conservation applied to the spherically symmetric tumour yields the following equation, which describes the evolution of the tumour radius:

$$\begin{aligned} \frac{d}{dt}\left(\frac{4}{3}\pi R^3\right) &= \int_{tumour} S(\sigma, \beta) r^2 dr d\theta d\phi, \\ \Rightarrow \frac{dR}{dt} &= \frac{1}{R^2}\int_0^{R(t)} S(\sigma, \beta) r^2 dr. \end{aligned} \tag{3}$$

We assume that the cell proliferation rate is a balance between the creation, or birth, of cells, and apoptosis, or cell death (see [19], [17], [18], [12] for a description of the structural changes involved in apoptosis). The inclusion of a natural cell loss mechanism distinguishes this work from that of, for example, [1], [6], [7]. Motivation for the inclusion of such a term stems from the existence of dormant tumour states, as discussed in the introduction.

In the absence of inhibitors, and assuming a first-order birth-rate ($s\sigma$) and a second-order death-rate ($-s\sigma^2/\tilde{\sigma}$) the following well-known logistic expression for $S(\sigma, \beta)$ can be obtained:

$$S(\sigma, \beta) = s\sigma\left(1 - \frac{\sigma}{\tilde{\sigma}}\right), \tag{4}$$

where $s, \tilde{\sigma}$ are constants. Regarding $(1 - \sigma/\tilde{\sigma})$ as an overcrowding factor, and assuming that the inhibitor acts in a similar manner, reducing the proliferation rate through overcrowding, the following composite rate is derived:

$$S(\sigma,\beta) = s\sigma\left(1-\frac{\sigma}{\tilde{\sigma}}\right)\left(1-\frac{\beta}{\tilde{\beta}}\right)$$

where $\tilde{\beta}$ is a constant, and cases for which both $\tilde{\sigma} < \sigma$ and $\tilde{\beta} < \beta$ at some point(s) inside the tumour are rejected as being physically unrealistic. At such points presence of the inhibitor transforms what, in the absence of the inhibitor, was a point of net cell loss into a point of net cell proliferation. Whilst this may explain some abnormal responses to anti-cancer drugs, it is not considered here since it runs counter to the prevailing interpretation of inhibitor action. Equally, we might consider

$$S(\sigma,\beta) = s\sigma\left(1-\frac{\sigma}{\tilde{\sigma}}\right)\left(1+\frac{\beta}{\tilde{\beta}}\right)^{-1},$$

so that the inhibitor simply reduces the magnitude of the proliferation rate, preserving its sign. For such separable proliferation rates ($S(\sigma,\beta) = \Sigma(\sigma)B(\beta)$), the inhibitor may be regarded as weighting the integrand, or point-wise proliferation rate, in (3). To simplify the analysis, throughout this paper attention is focussed on a proliferation rate which is linear with respect to both nutrient and inhibitor concentrations (this may be regarded as assuming a constant nutrient death rate). Thus we consider

$$S(\sigma,\beta) = s(\sigma-\tilde{\sigma})(1-\beta/\tilde{\beta}), \tag{5}$$

subject again to the physical constraint that $\tilde{\sigma} < \sigma$ and $\tilde{\beta} < \beta$ does not occur at any point inside the tumour. Other choices for $S(\sigma,\beta)$, such as those presented above, can be studied in a similar manner. Indeed, numerical results which employ the logistic proliferation rate (4) are included for comparison with (5).

As mentioned in the introduction, we are concerned only with *nonnecrotic*, phase I tumours. Following [1], [2], [5], [6], [20], we say that necrosis, or cell death, is initiated when the nutrient concentration falls below some (experimentally determined) value, σ_{nec} say. Where $\sigma < \sigma_{nec}$ cells no longer proliferate so that an additional factor $H(\sigma - \sigma_{nec})$ should be incorporated into $S(\sigma, \beta)$ to reflect this fact. Our stated intention to focus on phase I tumours means that henceforth attention is restricted to cases for which $\sigma > \sigma_{nec} \, \forall \, r \in [0, R]$.

We now prescribe boundary and initial conditions which close the system, and are chosen primarily to simplify the subsequent analysis. Symmetry of the tumour leads to the boundary conditions $\dfrac{\partial \sigma}{\partial r}(0,t) = 0 = \dfrac{\partial \beta}{\partial r}(0,t)$. In addition, we assume that both nutrient and inhibitor concentrations are prescribed on the tumour boundary so that $\sigma(R,t) = \sigma_R(t)$ and $\beta(R,t) = \beta_R(t)$. Initial nutrient and inhibitor concentration profiles $\sigma(r,0), \beta(r,0)$, together with an initial tumour radius $R(t=0)$ are prescribed. Equations (6)–(8) summarise these conditions:

$$\frac{\partial \sigma}{\partial r}(0,t) = 0, \;\; \sigma(R(t),t) = \sigma_R(t), \;\; \sigma(r,0) = \sigma_0(r), \tag{6}$$

$$\frac{\partial \beta}{\partial r}(0,t) = 0, \;\; \beta(R(t),t) = \beta_R(t), \;\; \beta(r,0) = \beta_0(r), \tag{7}$$

$$R(0) = R_0. \tag{8}$$

Functional forms for the interaction terms g_1, g_2 are now considered, recalling our interest in determining how different inhibitory mechanisms affect tumour growth. The paucity of experimental information available in the literature means that little is known about how inhibitors operate. For example, does an inhibitor function by destroying the nutritional value of some species or does it reduce the cell proliferation rate by modifying the cell DNA structure? Further, are there qualitative differences between these modes of operation? In an attempt to answer these questions, and following (5), several inhibitory mechanisms are now postulated.

- Inhibitor Free ($\beta \equiv 0$): $g_1 = 0 = g_2, S = s(\sigma - \tilde{\sigma})$.

- Inhibitor affects cell proliferation rate, not nutrient concentration: $g_1 = 0$, $g_2 = \gamma_2\beta$, $S = s(\sigma - \tilde{\sigma})(1 - \beta/\tilde{\beta})$.
- Inhibitor affects nutrient species, not cell proliferation rate: $g_1 = \gamma_1\beta, g_2 = \gamma_2\beta$, $S = s(\sigma - \tilde{\sigma})$.
- Inhibitor affects both nutrient concentration and cell proliferation rate: $g_1 = \gamma_1\beta$, $g_2 = \gamma_2\beta, S = s(\sigma - \tilde{\sigma})(1 - \beta/\tilde{\beta})$.

We remark here that, to simplify the analysis, we have assumed that the interaction terms $g_1(\sigma, \beta), g_2(\sigma, \beta)$ depend only on the inhibitor concentration, β. In this case, equation (2) decouples from the system, and β enters the reduced model as a prescribed forcing term in (1), and/or a renormalisation of the proliferation rate in (3). Whilst other expressions for g_1, g_2 which couple the two reaction-diffusion equations are probably more realistic, they are not discussed here since they are not amenable to simple analysis. Moreover, the results presented in sections 4 and 5 indicate that even these simple interaction terms give rise to realistic qualitative tumour behaviour.

Nondimensionalisation. Before continuing to determine steady solutions of equations (1)–(8), we express the moving boundary problem in a dimensionless form which leads naturally to an analysis using the method of multiple scales [21], [22], the two timescales being the tumour doubling time ($T \sim 1$ day) and the shorter, diffusion timescale ($R_0^2/D_1 \sim 1$ min). Defining independent variables $(\bar{r}, \bar{t}) = (r/R_0, t/T)$, and introducing the small parameter $0 < \epsilon = R_0^2/D_1T \ll 1$, the dependent variables and parameters are rescaled as follows

$$\bar{\sigma}(\bar{r}, \bar{t}) = \sigma(r, t)/\Sigma,\ \bar{\beta}(\bar{r}, \bar{t}) = \beta(r, t)/B,\ \bar{R}(\bar{t}) = R(t)/R_0, \tag{9}$$

$$(\bar{\sigma}_B, \bar{\sigma}_R, \bar{\sigma}_0, \bar{\tilde{\sigma}}) = \Sigma^{-1}(\sigma_B, \sigma_R, \sigma_0, \tilde{\sigma}),\ (\bar{\beta}_R, \bar{\beta}_0, \bar{\tilde{\beta}}) = B^{-1}(\beta_R, \beta_0, \tilde{\beta}), \tag{10}$$

$$\bar{D}_2 = D_2/D_1,\ \bar{\Gamma} = \Gamma R_0^2/D_1,\ \bar{\lambda} = \lambda R_0^2/D_1, \tag{11}$$

$$\bar{\gamma}_1 = \gamma_1 R_0^2 B/D_1\Sigma,\ \bar{\gamma}_2 = \gamma_2 R_0^2/D_1,\ \bar{S}(\bar{\sigma},\bar{\beta}) = S(\sigma,\beta)T, \tag{12}$$

where Σ is a typical nutrient concentration, such as $\max_{0\leq r\leq 1}\{\sigma_0(r)\}$, and B is a typical inhibitor concentration. Dropping the bars, the governing equations transform to give

$$\epsilon\frac{\partial\sigma}{\partial t} = \frac{1}{r^2}\frac{\partial}{\partial r}\left(r^2\frac{\partial\sigma}{\partial r}\right) + \Gamma(\sigma_B - \sigma) - \lambda\sigma - \gamma_1\beta, \tag{13}$$

$$\epsilon\frac{\partial\beta}{\partial t} = \frac{D_2}{r^2}\frac{\partial}{\partial r}\left(r^2\frac{\partial\beta}{\partial r}\right) - \gamma_2\beta, \tag{14}$$

$$\frac{\partial R}{\partial t} = \frac{s}{R^2}\int_0^R (\sigma - \tilde{\sigma})(1 - \beta/\tilde{\beta})r^2 dr, \tag{15}$$

subject to

$$\frac{\partial\sigma}{\partial r}(0,t) = 0,\ \sigma(R,t) = \sigma_R(t),\ \sigma(r,0) = \sigma_0(r), \tag{16}$$

$$\frac{\partial\beta}{\partial r}(0,t) = 0,\ \beta(R,t) = \beta_R(t),\ \beta(r,0) = \beta_0(r), \tag{17}$$

$$R(0) = 1. \tag{18}$$

3 Numerical Simulations

After transforming the moving boundary $r = R(t)$ to the fixed point $\rho = 1$ and rescaling the governing equations accordingly, equations (13)–(18) were solved numerically using finite-difference approximations [24]. The Crank-Nicolson method was used to solve the reaction-diffusion equations, whilst Simpson's rule was used to compute the integral in (15).

In addition to the estimate $\epsilon = 0.01$, derived in the previous section, a value of $D_2 = 0.5$ was adopted for the ratio of inhibitor to nutrient diffusion coefficient. This corresponds to cases for which the inhibitor molecules are more bulky, and, hence, diffuse less rapidly, than the nutrient molecules. In the absence of relevant experimental data, $O(1)$-estimates were adopted for the remaining dimensionless parameters.

3.1 Inhibitor-Free Simulations

Figures 1 to 4 summarise the range of qualitative behaviour obtained from the inhibitor-free simulations ($\beta = 0$). When the linearly-dependent proliferation rate was employed two possible outcomes were observed. In the first case, irrespective of the initial tumour radius, the nutrient concentration rapidly adopted a constant profile ($\sigma = \sigma_R \forall\ r \in [0, R(t)]$), whilst the tumour radius decayed monotonically, eventually disappearing altogether. The alternative outcome showed the nutrient concentration rapidly attaining a nontrivial, monotonically increasing profile, and, depending on its initial value, the tumour radius increasing, or decreasing, to an equilibrium value, the limiting radius independent of the starting radius. Typical examples of each mode of behaviour are reproduced in figures 1 and 2. From the simulations we observed that the type of behaviour which results is strongly dependent on the ratio $\tilde{\sigma}/\sigma_R$: as the external nutrient concentration σ_R increases decay of the tumour to zero is superceded by evolution of the tumour to a radius of finite size. (Discussions of the existence and stability of steady-state tumour configurations in the following sections render this result more explicit.)

The importance that the functional form of the proliferating rate has on the evolution of the tumour becomes apparent when we contrast the above behaviour with that observed when the linear proliferating rate is replaced by a logistic term (4). Again, two possible outcomes may result: either the tumour radius decays away to zero, or it increases without bound. For sufficiently large values of $\tilde{\sigma}$ the tumour radius increases unboundedly, regardless of its initial value. However, for smaller values of $\tilde{\sigma}$, disappearance of the tumour may occur, provided the initial tumour radius is 'small enough'. These types of behaviour are reproduced in figures 3 and 4, and, together with figures 1 and 2, demonstrate how important accurate knowledge of the proliferating rate is when assessing the behaviour of a tumour.

3.2 Inhibitor-Present Simulations

The model equations (13)-(18) introduced two mechanisms for inhibitor action: either as a sink of nutrient in (13) (indirect action), or as a reduction in the cell proliferation rate in (16) (direct action). For comparison with the inhibitor-free results presented above, we examine the effect that these modes of action, taken separately and together, have on the tumour's development. Tables 1 and 2 below summarise these results, showing the variation of the equilibrium tumour radius R_∞ on the mode of inhibitor action for a typical data set. With $\tilde{\sigma} = 0.6$, Table 1 shows that both the direct and indirect modes of action have the capacity to reduce the size of the dormant tumour. With the inhibitor action in both manners ($\gamma_1 = 1.0, \tilde{\beta} = 0.95$), a change in the qualitative behaviour of the system occurs, with the appearance of two attraction states ($R_\infty = 2.10,\ 0.00$). From figure 5 we observe that if, prior to the introduction of the inhibitor, the tumour is sufficiently small (here, $R(0) < 0.7$) then the tumour will actually disappear. For larger initial radii, as before, the tumour evolves to a finite size. Referring now to Table 2, with $\tilde{\sigma} = 1.1$, stability of the inhibitor-free configuration is maintained if the inhibitor acts indirectly ($\gamma_1 = 1.0, \tilde{\beta} = 10.0$). However, direct action of the inhibitor introduces a stable, nontrivial configuration (see figure 6). Thus, in this case, treatment with the inhibitor actually exacerbates the situation.

Table 1

	$\tilde{\sigma}$	γ_1	$\tilde{\beta}$	R_∞
	0.6	0.0	$+\infty$	4.75
	0.6	0.1	10.00	4.50
	0.6	0.1	0.95	3.30
	0.6	1.0	10.00	3.00
(Fig 5)	0.6	1.0	0.95	2.10, 0.00

Table 2

	$\tilde{\sigma}$	γ_1	$\tilde{\beta}$	R_∞
	1.1	0.0	$+\infty$	0.00
	1.1	0.1	10.00	0.00
	1.1	0.1	0.95	0.60
	1.1	1.0	10.00	0.00
(Fig 6)	1.1	1.0	0.95	0.53

4 Steady Solutions

The numerical results of the previous section indicate how both the parameter values and the functional forms employed in the model affect a tumour's subsequent growth. For example, for the inhibitor-free model, the existence of a nontrivial steady solution is predicted in figure 2. In this section time-independent solutions of equations (13)–(18) are sought, and bounds within which these nontrivial solutions exist are determined, analytically for the inhibitor-free model, and numerically for the inhibitor-present models. The stability of the steady solutions is then addressed in section 5, where the governing equations are analysed using the method of multiple-scales.

4.1 Inhibitor-Free Analysis

With $\beta \equiv 0$, and $S(\sigma, \beta) = s(\sigma - \tilde{\sigma})$, setting $\dfrac{\partial}{\partial t} \equiv 0$ in (13)–(18) yields the inhibitor-free steady-state model satisfied by $(\sigma, R) = (\sigma_S(r), R_S)$.

$$0 = \frac{1}{r^2}\frac{\partial}{\partial r}\left(r^2 \frac{\partial \sigma_S}{\partial r}\right) + \Gamma(\sigma_B - \sigma_S) - \lambda \sigma_S, \tag{19}$$

$$\frac{\partial \sigma_S}{\partial r}(0) = 0, \sigma_S(1) = \sigma_{R_S}, \tag{20}$$

$$\int_0^{R_S} \sigma_S r^2 dr = \frac{\tilde{\sigma} R_S^3}{3}. \tag{21}$$

In (19)–(21) the initial conditions are now redundant. We denote by σ_{nec} the threshold nutrient concentration below which necrosis occurs, and remark that if $\tilde{\sigma} < \sigma_{nec}$ then, for a nontrivial solution, there exists some neighbourhood $[r_L, r_U] \subset [0, R_S]$ such that $\sigma_S(r) < \sigma_{nec}\ \forall\ r \in [r_L, r_U]$. Thus necrosis is predicted inside the tumour and no phase I solutions exist. We conclude that an overall death rate of nutrient cells in excess of some critical value ($\tilde{\sigma} > \sigma_{nec}$, in our notation) is essential for obtaining nontrivial steady solutions which do not possess necrotic cores. This highlights the important role of apoptosis in explaining the existence of those dormant tumours observed in vitro and in vivo [16], [11].

Solving (19), subject to (20), we obtain the following solution for $\sigma_S(r)$:

$$\sigma_S = \frac{\Gamma \sigma_B}{\Gamma + \lambda} + \frac{A_S}{r} \sinh \sqrt{\Gamma + \lambda}\, r, \tag{22}$$

where $A_S = R_S(\sigma_{R_S} - \Gamma\sigma_B/(\Gamma+\lambda))/\sinh\sqrt{\Gamma+\lambda}R_S$. From (22) we note that the nutrient concentration attains its extrema at $\rho = 0, 1$, the nature of these points characterised by the sign of A_S, or, equivalently, the balance between the nutrient consumption rate ($\lambda\sigma_{R_S}$) and the rate of nutrient transfer from the vasculature to the tumour cells on the tumour boundary ($\Gamma(\sigma_B - \sigma_{R_S})$):

- $A_S > 0 \Leftrightarrow \lambda\sigma_{R_S} > \Gamma(\sigma_B - \sigma_{R_S}) \Rightarrow$ necrosis emanates from $\rho = 0$;
- $A_S < 0 \Leftrightarrow \lambda\sigma_{R_S} < \Gamma(\sigma_B - \sigma_{R_S}) \Rightarrow$ necrosis emanates from $\rho = 1$.

The prediction of necrosis at the tumour periphery is a consequence of assuming the tumour is vascular: for an avascular tumour ($\Gamma = 0$), $A_S > 0$, so that, if it occurs, necrosis originates from $r = 0$. Since in our model the nutrient concentration is prescribed on $r = R$ then, tautologically, $\sigma_R < \sigma_{nec}$ is a necessary condition for necrosis to emanate from $r = R$. For a less obvious result a mixed boundary condition of the form $\dfrac{\partial \sigma}{\partial r}(R, t) \propto [\sigma_B - \sigma(R, t)]$ should be imposed in place of (20). Whilst both of the above cases are observed in practice

[16], most authors [1], [2], [5], [15], [20] have only considered situations in which necrosis appears at the tumour centre. Indeed, to our knowledge, only [1] and [25] have studied the case where necrosis is initiated at the tumour periphery, using it to describe the development of in vivo tumour chords.

Imposing the integral constraint (21), which derives from (15) when $\frac{\partial}{\partial t} = 0$, we obtain the following, implicit expression for R_S, which can be solved numerically:

$$\tanh \eta = \frac{\eta}{1 + \Lambda \eta^2}, \tag{23}$$

$$\text{where } \Lambda = \frac{1}{3}\left\{\tilde{\sigma} - \frac{\Gamma \sigma_B}{\Gamma + \lambda}\right\} \Big/ \left\{\sigma_{R_S} - \frac{\Gamma \sigma_B}{\Gamma + \lambda}\right\} \text{ and } \eta = \sqrt{\Gamma + \lambda} R_S. \tag{24}$$

From (23) it is clear that η depends only on the parameter grouping Λ so that $R_S = \eta / \sqrt{\Gamma + \lambda}$ depends on both Λ and $\sqrt{\Gamma + \lambda}$. Figure 7 illustrates the variation of η with Λ, with Γ and λ held fixed. From this diagram we deduce that, for fixed values of Γ and λ, increases in Λ, brought about by increases in $\tilde{\sigma}$ or reductions in either σ_B or σ_{R_S}, give rise to smaller steady-state tumour radii. Increasing λ, or decreasing Γ, whilst holding the other parameters fixed, leads to similar reductions in the steady-state radius. We remark also that the trivial solution $R_S = 0$ is a root of (23). Further, in figure 7, nontrivial solutions for η, or R_S, exist only for a finite range of Λ: outside this domain no nontrivial steady solutions exist. These remarks are made more precise in the following lemma, in which necessary conditions for the existence of nontrivial steady solutions are presented.

Lemma 1 *If* $0 < \tilde{\sigma} < \sigma_{R_S}$ *then* $0 < \Lambda < 1/3$, *and there exists a unique* $\eta > 1/\sqrt{\Lambda}$ *which satisfies (23). Moreover, a nontrivial solution to (19)–(21) exists for which the outer radius of the tumour satisfies* $R_S > 1/\sqrt{\Lambda(\Gamma + \lambda)}$.

Proof. Consider the functions $f_1(y) = \tanh y$ and $f_2(y) = y/(1 + \Lambda y^2)$ so that nontrivial steady tumour configurations correspond to positive roots $\Delta f(y) = f_1 - f_2 = 0$. The restriction to $\Lambda > 0$ follows naturally when we note that if $\Lambda < 0$ then

$$0 < f_1 < f_2 \; \forall \; y \in \; (0, 1/\sqrt{\Lambda}] \text{ and } f_2 < 0 < f_1 \; \forall \; y \in \; (1/\sqrt{\Lambda}, \infty).$$

Since f_1 increases monotonically from 0 to 1 whilst, for $\Lambda > 0$, f_2 increases to a unique maximum at $y = 1/\sqrt{\Lambda}$ and then tends monotonically to zero, a necessary condition for existence of a unique root $y^* > 1/\sqrt{\Lambda}$ is that f_2 increases more rapidly than f_1 as y increases from zero. Now, at the origin,

$$\Delta f(0) = \Delta f'(0) = \Delta f''(0) = 0, \Delta f'''(0) = 6(\Lambda - 1/3),$$

and the result follows. □

The bound on Λ can be strengthened further by imposing the additional constraint $\min\{\sigma_S(0), \sigma_S(R_S)\} > \sigma_{nec}$ which ensures that necrosis has not occurred, since, by the maximum principle, σ attains its minimum value at either $r = 0$ or $r = R_S$.

At first sight, Lemma 1 may appear to contradict results reported by Greenspan *et al.* [1], [2], [6], [20] whose models predict exponential growth of the tumour throughout phase I, until a necrotic core develops with the onset of phase II. Now, as mentioned earlier, experimental results [11], [12] indicate that tumours do not always develop necrotic cores, whilst Lemma 1 provides a basis for establishing conditions under which such non-necrotic solutions might be realised. Further, if $\tilde{\sigma} = 0$, then $|\Lambda| > 1/3$, and the bounds of Lemma 1 are violated. Thus, no steady-state solutions occur when no death term is included in the cell proliferation rate $S(\sigma, \beta)$, and the results of Greenspan *et al.* are recovered. In summary, as claimed in the introduction, the inclusion in our model of apoptosis is crucial to obtaining nontrivial, steady, phase I tumour configurations.

Before examining the effect of the steady-state tumour radius caused by the presence of an inhibitor, and to simplify the analysis, we assume henceforth that $\Gamma = 0$ in (13). In this case the bound on Λ derived in Lemma 1 reduces to $0 < \tilde{\sigma} < \sigma_R$ and the resulting steady-state tumours possess a quasi two-layer structure, with cell proliferation occurring in the outer region where $\tilde{\sigma} < \sigma < \sigma_R$, cell death towards the centre of the tumour where $\sigma < \tilde{\sigma}$, and the two effects, averaged over the tumour, in equilibrium.

4.2 Inhibitor-Present Analysis

For the general (dual-action) inhibitor-present case, in which the inhibitor acts by reducing nutrient levels inside the tumour and also by reducing the cell proliferation rate, steady solutions of equations (13)–(18), with $\Gamma = 0$, have the following nutrient and inhibitor profiles:

$$\sigma_S = \frac{A_S \sinh \sqrt{\Gamma + \lambda} r}{r} + \frac{\Delta B_S \sinh \theta r}{r}, \;\; \beta_S = \frac{B_S \sinh \theta r}{r},$$

where

$$\Delta = \frac{\gamma_1}{\gamma_2 / D_2 - \lambda}, \;\; \theta^2 = \frac{\gamma_2}{D_2}, \;\; A_S = \frac{(\sigma_{R_S} - \Delta \beta_{R_S}) R_S}{\sinh \eta}, \;\; B_S = \frac{\beta_{R_S} R_S}{\sinh \theta R_S}.$$

Applying conservation of mass, through (16), leads to the following implicit expression for $\eta = \sqrt{\lambda} R_S$, which is the inhibitor-present analogue of (23):

$$\begin{aligned} 0 = {} & (1 - \Lambda_1) \left(\frac{\eta}{\tanh \eta} - 1 \right) - \Lambda_0 \eta^2 + \frac{(3\Lambda_0 \Lambda_2 + \Lambda_1)}{\phi^2} \left(\frac{\phi \eta}{\tanh \phi \eta} - 1 \right) \\ & - \frac{\Lambda_2 (1 - \Lambda_1)}{(\phi^2 - 1)} \left(\frac{\phi \eta}{\tanh \phi \eta} - \frac{\eta}{\tanh \eta} \right) - \frac{\Lambda_1 \Lambda_2 \eta}{\phi \tanh \phi \eta} + \frac{\Lambda_1 \Lambda_2 \eta^2}{2 \sinh^2 \phi \eta}, \end{aligned} \tag{25}$$

where

$$\Lambda_0 = \frac{\tilde{\sigma}}{3 \sigma_{R_S}}, \;\; \Lambda_1 = \frac{\Delta \beta_{R_S}}{\sigma_{R_S}}, \;\; \Lambda_2 = \frac{\beta_{R_S}}{\tilde{\beta}}, \;\; \phi^2 = \frac{\theta^2}{\lambda} = \frac{\gamma_2}{D_2 \lambda}.$$

The effect on the steady-state radius of the three inhibitory mechanisms postulated in section 2 can be compared using (25). For example, with $\gamma_1 = 0 = \Lambda_1$ in (25), so that the inhibitor acts directly on the cell proliferation rate, $\eta = \sqrt{\lambda} R_S$ is given by:

$$0 = \left(\frac{\eta}{\tanh \eta} - 1\right) - \Lambda_0 \eta^2 + \frac{3\Lambda_0 \Lambda_2}{\phi^2}\left(\frac{\phi\eta}{\tanh \phi\eta} - 1\right) - \frac{\Lambda_2}{(\phi^2 - 1)}\left(\frac{\phi\eta}{\tanh \phi\eta} - \frac{\eta}{\tanh \eta}\right). \quad (26)$$

Similarly, in the limit $\tilde{\beta} \to \infty$, with $\Lambda_2 = 0$, the inhibitor acts indirectly via the nutrient reaction-diffusion equation, and $\eta = \sqrt{\lambda} R_S$ satisfies:

$$0 = (1 - \Lambda_1)\left(\frac{\eta}{\tanh \eta} - 1\right) - \Lambda_0 \eta^2 + \frac{\Lambda_1}{\phi^2}\left(\frac{\phi\eta}{\tanh \phi\eta} - 1\right). \quad (27)$$

Figures 8(a,b,c) illustrate the range of effects that the modes of direct and indirect inhibitor action postulated here may induce on η, as defined by equations (25)–(27). Thus, in figure 8(a) a smaller steady-state radius is predicted in the presence of a dual-action inhibitor. Cases for which the inhibitors act either directly or indirectly are not shown on the diagram – they yield radii which are bounded above and below by the inhibitor-free and inhibitor-present radii. In figure 8(b), existence of the dual-action, inhibitor-present solutions is restricted to a smaller range of values of Λ_0 than for the inhibitor-free case. Where they exist, yet again, smaller steady-state radii are predicted. However, they are no longer unique, with two possible configurations for each value of Λ_0. In figure 8(c) the three different modes of inhibitor action are compared with the inhibitor-free case as the parameter Λ_1 varies.

These results highlight some of the difficulties associated with prescribing anticancer drugs to patients. For example, from figure 8(c) we observe that the benefits of administering a direct or indirect action inhibitor are strongly dependent on the parameter Λ_1. In addition, the restriction of steady solutions to smaller parameter regimes, together with the prediction of multiple steady states, that result from addition of an inhibitor force us to question the stability of these steady configurations. For example, if, where no nontrivial solutions exist, the trivial solution is stable then treatment with an inhibitor which reduces the domain of existence of nontrivial solutions necessarily increases the size of the domain in which the tumour will disappear. In such cases, the inhibitor acts beneficially. However, if the trivial solution is unstable where no nontrivial solutions exist (cf figure 3, in which a logistic proliferation rate was employed), then it is possible that treatment with an inhibitor may lead to unbounded growth of a previously stable tumour. In the next section we discuss how to assess the stability of the steady solutions in order that these problems may be resolved.

5 Stability Analysis

Reverting once more to inhibitor-free analysis, we recall that nontrivial steady solutions to (13)–(18) exist for $0 < \Lambda < 1/3$, the range specified in Lemma 1, whilst trivial solutions exist for all parameter values. In this section we attempt to determine whether such states would be observed in practice through a stability analysis based on the method of multiple scales [21], [22]. As mentioned in the introduction, motivation for adopting such an approach stems from the existence of two natural timescales associated with tumour growth, namely the tumour's doubling time ($T \sim 1$ day) and the shorter, nutrient diffusion timescale ($R_0^2/D_1 \sim 1$ min). A steady state is said to be asymptotically stable if, given an initial tumour configuration, defined by $\sigma(r,0)$ and $R(0)$, the steady-state is recovered as $t \to \infty$ in equations (13)–(18).

Introducing the fast time $\tau = t/\epsilon$, where $0 < \epsilon = R_0^2/D_1 T \ll 1$, we seek solutions to (13)–(18) in which the timescales t, τ figure as independent variables so that, with $\beta = 0$, (σ, R) now satisfy

$$\epsilon \frac{\partial \sigma}{\partial t} + \frac{\partial \sigma}{\partial \tau} = \frac{1}{r^2}\frac{\partial}{\partial r}\left(r^2 \frac{\partial \sigma}{\partial r}\right) - \lambda \sigma, \tag{28}$$

$$\frac{\partial R}{\partial t} + \frac{1}{\epsilon}\frac{\partial R}{\partial \tau} = \frac{s}{R^2}\int_0^R (\sigma - \tilde{\sigma}) r^2 dr, \tag{29}$$

subject to

$$\frac{\partial \sigma}{\partial r}(0, t, \tau) = 0,\ \sigma(R, t, \tau) = \sigma_R,\ \sigma(r, 0, 0) = \sigma_0(r), \tag{30}$$

$$R(0, 0) = 1. \tag{31}$$

A perturbation expansion is performed by writing

$$\begin{aligned} \sigma(r, t, \tau) &= \sigma_0(r, t, \tau) + \epsilon\sigma_1(r, t, \tau) + \ldots, \\ R(t, \tau) &= R_0(t) + \epsilon R_1(t, \tau) + \ldots, \end{aligned}$$

where we have already noted that, to leading order, R is independent of τ. The leading order expression for σ_0 is given by

$$\sigma_0 = \frac{A_0(t)\sinh\sqrt{\lambda}r}{r} + \frac{1}{r}\sum_n A_n(t) e^{-\omega_n^2\tau}\sin\left(\frac{n\pi r}{R_0(t)}\right);$$

where $\omega_n^2 = n^2\pi^2 + \lambda$,

$$A_0(t) = \frac{\sigma_R R_0(t)}{\sinh\sqrt{\lambda}R_0(t)},$$

and the Fourier coefficients satisfy

$$A_n(0) = \frac{2}{R_0(0)}\left\{\int_0^{R_0(0)} \sigma_0(r)\sin\left(\frac{n\pi r}{R_0(0)}\right) r dr + \frac{(-1)^n R_0(0)}{n\pi}\sinh\sqrt{\lambda}R_0(0)\right\}.$$

Equating to zero coefficients of $O(1)$ in (29) then yields

$$\begin{aligned}\frac{\partial R_1}{\partial \tau} &= \frac{s}{R_0^2}\int_0^{R_0}(\sigma_0-\tilde{\sigma})r^2 dr - \frac{dR_0}{dt},\\ &= F(t) + s\sum_n A_n(t)e^{-\omega_n^2\tau}\int_0^{R_0} r\sin\left(\frac{n\pi r}{R_0(t)}\right)dr,\end{aligned}$$

where the function $F(t)$ is defined by

$$F(t) = \frac{s}{R_0^2}\int_0^{R_0} A_0(t) r \sinh\sqrt{\lambda} r dr - \frac{s\tilde{\sigma}R_0}{3} - \frac{dR_0}{dt}.$$

For a uniform expansion, valid at least for $t \leq O(\epsilon^{-1})$, we set $F(t) \equiv 0$ which, on rearrangement, supplies the following expression for $\eta = \sqrt{\lambda}R_0(t)$:

$$\frac{1}{s\sigma_R}\frac{d\eta}{dt} = \frac{1}{\tanh\eta} - \frac{1}{\eta} - \Lambda\eta, \tag{32}$$

where $\Lambda \equiv \Lambda_0 = \dfrac{\tilde{\sigma}}{3\sigma_R}$. Imposing $\dfrac{d}{dt} = 0$ in (32), equation (23), the implicit expression for the steady-state tumour radius in the absence of inhibitors, is recovered. We can now deduce the stability of the trivial and, where they exist, nontrivial steady-states, using (32) to sketch trajectories in $(\eta, \dfrac{d\eta}{dt})$-space for different values of Λ – the steady-state is said to be stable if it is recovered in the limit as $t \to \infty$ in (32); otherwise the steady-state is unstable. From the profiles presented in figure 9 it is clear that, subject to the above interpretation of stability, where it exists, the nontrivial solution is stable whilst the trivial solution is stable only if $\Lambda > 1/3$, that is where no nontrivial solutions exist. The latter result can also be deduced by taking the limit $\eta \to 0$ in (32):

$$\lim_{\eta\to 0}\frac{1}{s\sigma_R}\frac{d\eta}{dt} = \frac{(1-3\Lambda)}{3}\eta.$$

The above results are summarised in figure 10 where the limiting tumour radius R_∞ is plotted against the parameter Λ.

Applying the above method of two-timing analysis to the inhibitor models presented in sections 3 and 4 we can also assess the effect an inhibitor has on the stability of the predicted steady-state configurations. For the general inhibitor-present case ($S(\sigma,\beta) = s(\sigma-\tilde{\sigma})(1-\beta/\tilde{\beta})$, $\gamma_1,\gamma_2>0$), the analogue of (32), which describes the evolution of the tumour radius to leading order, is given by:

$$\begin{aligned}\frac{1}{s\sigma_R}\frac{d\eta}{dt} &= (1-\Lambda_1)\left(\frac{1}{\tanh\eta}-\frac{1}{\eta}\right)-\Lambda_0\eta+\frac{(3\Lambda_0\Lambda_2+\Lambda_1)}{\phi}\left(\frac{1}{\tanh\phi\eta}-\frac{1}{\phi\eta}\right)\\ &-\frac{\Lambda_2(1-\Lambda_1)}{(\phi^2-1)}\left(\frac{\phi}{\tanh\phi\eta}-\frac{1}{\tanh\eta}\right)-\frac{\Lambda_1\Lambda_2}{\phi\tanh\phi\eta}+\frac{\Lambda_1\Lambda_2\eta}{2\sinh^2\phi\eta}. \end{aligned} \tag{33}$$

As expected, setting $d\eta/dt \equiv 0$ we recover equation (25), which defines the steady-state tumour radius in the presence of an inhibitor. Sketches of (33) for different values of the governing parameters show that, as for the inhibitor-free case, where a unique nontrivial steady solution exists it is stable and also that where no nontrivial solutions exist the trivial solution is stable. However the appearance of a second, (unstable) nontrivial solution partitions the system into two stable domains, depending on whether the tumour is initially larger, or smaller, than the intermediate value: tumours with smaller radii are attracted to the trivial solution whilst those with larger radii are attracted to the larger (stable) nontrivial solution. Analysis of (33) in the limit $|\eta| \ll 1$ provides some insight into when this situation arises.

$$\lim_{\eta\to 0}\frac{1}{s\sigma_R}\frac{d\eta}{dt} = \frac{(1-3\Lambda_0)(1-\Lambda_2)}{3}\,\eta.$$

so that if $\Lambda_0 \in (0,1/3)$ and $\Lambda_2 \in (0,1)$ then the trivial solution is unstable whereas if $\Lambda_2 > 1$ then the trivial state is stable. Thus, we conclude that uniqueness of the nontrivial steady-state is violated when $\Lambda_2 > 1$, a result which is consistent with the numerical simulations presented in figures 8(a,b,c): nonunique solutions are predicted only for those cases having $\Lambda_2 > 1$.

6 Conclusions

In this paper the range of application of existing models of solid tumour growth has been extended through the inclusion of a vascular exchange term and a natural cell loss mechanism known as apoptosis. Thus, whilst the models of Adam, Greenspan and others [1], [2], [5], [6] have particular relevance to situations where multicell spheroids are grown in isolation in petri dishes, it is anticipated that the model presented here may be used to describe not only the growth of such in vitro cancers but also to describe the development of in vivo avascular and vascular tumours. This extended range of tumour configurations leads, in turn, to a discussion of a wider class of inhibitory mechanisms. For example, we contrast the efficacy of inhibitors which act indirectly by reducing the nutritional value of some species (σ) with that of inhibitors which act directly by modifying the cell proliferation rate ($S = S(\sigma, \beta)$). A further distinguishing feature of this work arises from the treatment of the two timescales associated with tumour growth. Existing work neglects the shorter, nutrient diffusion timescale and focusses on the longer, tumour doubling timescale. Here, however, variation of the dependent variables on both timescales is permitted. This distinction enables us to gain insight into the previously unstudied, transient behaviour of tumours, without affecting the longer timescale dynamics, or the nature of the steady solutions. In addition, stability of the steady configurations can be assessed by recasting the problem in a form suitable for two-timing analysis [22], [21].

Numerical simulations of the resulting model, in the absence of any inhibitor ($\beta \equiv 0$), show two characteristic modes of tumour growth: the tumour either shrinks in size, and eventually disappears (stability of the trivial solution), or else its radius asymptotes to a nonzero value (stability of the nontrivial solution). A study of the existence and stability of such steady solutions supports these numerical results and enables us to predict, a priori, the growth pattern of a given tumour, the outcome depending on the size of a single parameter grouping Λ, which is defined in terms of the system parameters. In particular, if $\Lambda > 1/3$ then the trivial solution is asymptotically stable, and no nontrivial tumours exist. Conversely, if $0 < \Lambda < 1/3$ then the trivial solution is unstable and a nontrivial tumour configuration exists which is stable. For an avascular tumour ($\Gamma = 0$), this result reduces to give $0 < \tilde{\sigma} < \sigma_R$ as necessary conditions for the existence, and stability, of nontrivial tumour configurations. From this we deduce the important role played by apoptosis in obtaining nontrivial solutions: in the absence of apoptosis, with $\tilde{\sigma} = 0$, the trivial solution is the only steady solution. Where they exist, the steady solutions possess a quasi two-layer structure: in the outer region there is a net proliferation of cells, towards the centre of the tumour there is a net loss of cells, but the net result of the two effects, averaged over the tumour, yields an equilibrium configuration.

Modifications to the characteristic growth pattern may be effected both by adapting the functional form of the proliferating rate and by introducing an inhibitory species into the tumour. For example, using a logistic proliferating rate unbounded growth of the tumour may result (instability of the trivial steady solution) for all tumours. By decreasing the carrying capacity $\tilde{\sigma}$ in the logistic term the appearance of an unstable nontrivial steady solution, having radius R_U say, is concomitant with the creation of a finite basin of attraction of the trivial solution: if the tumour radius is initially smaller than R_U then the tumour disappears; otherwise, unbounded growth results. Inclusion of an inhibitor may induce a similar change in the stability of the trivial solution in cases for which the inhibitor-free model admits stable nontrivial solutions. Here the appearance of a second unstable nontrivial solution separates the stable nontrivial configuration from a stable tumour-free configuration.

The results presented in this paper, and discussed above, pertain to an admittedly simple model of tumour growth, with scope for further improving and extending the model. For example, similar analyses could be applied to models of more highly differentiated structures, possessing developed necrotic cores and which distinguish between the cell density and the nutrient concentration (cf. [26] - [35]). In addition, the effect of imposing more biologically realistic boundary conditions should be investigated. Given the importance of the functional form of the proliferation rate on the development of a tumour, it seems particularly important to use experimental data to estimate realistic expressions for $S(\sigma, \beta)$ and other interaction terms. The decision to employ simpler expressions here was taken in order to focus attention on describing a methodological approach for studying tumour growth, which can easily be adapted to a particular application. Whilst this would, in general, entail only numerical simulations, we hope that, by demonstrating the existence and stability of nontrivial tumours for our simplistic model, some insight into the generic behaviour of tumour and their treatment can be derived.

We now, therefore, discuss the implications, and potential application, of our results to the understanding and treatment of cancer. Firstly, on the basis of our inhibitor-free simulations and analysis, we propose the following explanation for the natural disappearance of the small malignancies which frequently occur in man. Under normal circumstances the tissue environment is hostile to the malignancy ($\Lambda > 1/3$, in our notation), and the tumour-free trivial state is the only stable configuration that can be sustained. A change in the tissue environment brought about by, for example, stress, illness or disease, transforms the system into one which is more conducive to tumour growth ($0 < \Lambda < 1/3$, for the inhibitor-free case). Depending on the physical laws governing nutrient consumption, cell proliferation, etc., the tumour may develop rapidly and without bound until compressional forces from the external surroundings of the host organ check its growth (unstable growth). Equally, it may grow to a finite size (existence and stability of nontrivial solution) which is relatively harmless to the individual and can be sustained until either the tumour becomes vascularised, as a result of angiogenesis, or until some change in the external surroundings destabilises the dormant configuration. Through an understanding of the balance of physical effects which characterises a tissue environment as either hostile or susceptible to cancers, it should be possible to devise strategies which, by altering the system's parameters, stabilise the system and, therefore, prevent tumours from persisting. For the inhibitor-free analysis presented here, this would correspond to maintaining $\Lambda > 1/3$. In practice, physico-chemical constraints will dictate how such an affect may most easily be achieved – for example, recalling the definition of Λ, possibly by reducing the vascular delivery of nutrients (Γ), or by reducing the external nutrient concentration ($\tilde{\sigma}$). The inhibitor-present analysis provides a further explanation of the disappearance of malignancies, driven by an immune response in the host tissue. In this case, secretion of an inhibitory species on the host tissue may render the tissue environment once more hostile to the tumour which, as a result, disappears. Referring to Table 2, we remark that activation of the immune system may in certain, abnormal cases lead to the appearance of a dormant steady-state where, in the absence of the inhibitor, the trivial state is stable. Interpreting the inhibitor instead as a drug used in the treatment of cancer demonstrates the need to ensure that beneficial operating conditions are maintained. For example, a patient with two tumours of differing sizes, treated with an anticancer drug, may find that whilst the smaller, less harmful tumour disappears, the larger one actually grows in size (figure 5).

References

[1] J.A. Adam, A simplified mathematical model of tumour growth, *Math. Biosci.* 81:229-244 (1986).

[2] J.A. Adam, A mathematical model of tumour growth. II. Effects of geometry and spatial uniformity on stability, *Math. Biosci.* 86:183-211 (1987).

[3] J.A. Adam, A mathematical model of tumor growth III: Comparison with experiment, *Math. Biosci.* 86:213-227 (1987).

[4] J.A. Adam, Corrigendum: A mathematical model of tumor growth by diffusion, *Math. Biosci.* 94:155 (1989).

[5] J.A. Adam and S.A. Maggelakis, Diffusion regulated growth characteristics of a spherical prevascular carcinoma, *Bull. Math. Bio.* 52:549-582 (1990).

[6] H.P. Greenspan, Models for the growth of a solid tumour by diffusion, *Stud. Appl. Math.* 52:317-340 (1972).

[7] S.A. Maggelakis and J.A. Adam, Mathematical model of prevascular growth of a spherical carcinoma, *Math. Comput. Modelling* 13:23-38 (1990).

[8] G. Adam, U. Steiner, H. Maier and S. Ulrich, Analysis of cellular interactions in density-dependent inhibition of 3T3 cell proliferation, *Biophys. Struct. Mech.* 9:75-82 (1982).

[9] J.P. Freyer and R.M. Sutherland, Regulation of growth saturation and development of necrosis in EMT6/Ro multicellular spheroids by the glucose and oxygen supply, *Cancer Res.* 46:3504-3512 (1986).

[10] J.P. Freyer and R.M. Sutherland, Proliferative and clonogenic heterogeneity of cells from EMT6/Ro multicellular spheroids induced by the glucose and oxygen supply, *Cancer Res.* 46:3513-3520 (1986).

[11] R.M. Sutherland and R.E. Durand, Radiation response of multicell spheroids - an in vitro tumour model, *Internat. J. Radiat. Biol.* 23:235-246 (1973).

[12] M. Tubiana, The kinetics of tumour cell proliferation and radiotherapy, *Br. J. Radiol.* **44**, 325-347 (1971).

[13] J. Folkman and M. Hochberg, Self-regulation of growth in three dimensions, *J. Exp. Med.* 138:745-753 (1973).

[14] M.A.J. Chaplain, Mathematical models for the growth of solid tumours and the tip morphogenesis of *Acetabularia*. Ph.D. Thesis, University of Dundee (1990).

[15] J. Folkman, Tumour angiogenesis, *Adv. Cancer Res.* 19:331-338 (1974).

[16] J. Folkman, The vascularisation of tumours, in *Cancer Biology, Scientific American*, E.C. Friedberg, ed., pp. 115-124 (1976).

[17] J.F.R. Kerr, Shrinkage necrosis; a distinct mode of cellular death, *J. Path.* 105:13-20 (1971).

[18] J.F.R. Kerr, A.H. Wyllie and A.R. Currie, Apoptosis: a basic biological phenomenon with wide-ranging implications in tissue kinetics, *Br. J. Cancer* 26:239-257 (1972).

[19] R.E. Durand, Cell cycle kinetics in an *in vitro* tumour model, *Cell Tissue Kinet.* 9:403-412 (1976).

[20] D.L.S. McElwain and L.E. Morris, Apoptosis as a volume loss mechanism in mathematical models of solid tumour growth, *Math. Biosci.* 39:147-157 (1978).

[21] D.W. Jordan and P. Smith, *Nonlinear ordinary differential equations*, Clarendon Press, Oxford, 1977.

[22] A.H. Nayfeh, *Perturbation methods*, John Wiley and Sons, Inc., 1973.

[23] M.A.J. Chaplain and N.F. Britton, On the concentration profile of a growth inhibitory factor in multicell spheroids, *Math. Biosci.* 115:233-245 (1993).

[24] G.D. Smith, *Numerical solution of partial differential equations: finite difference methods*, Clarendon Press, 1985.

[25] D.L.S. McElwain and G. Pettet, Cell migration in multicell spheroids: swimming against the tide, *Bull. Math. Biol.* 55:655-674 (1993).

these references need to be incorporated into text

[26] R.E. Durand, Multicell spheroids as a model for cell kinetic studies, *Cell Tissue Kinet.* 23:141-159 (1990).

[27] J.P. Freyer, E. Tustanoff, A.J. Franko and R.M. Sutherland, In situ oxygen consumption rates of cells in V-79 multicellular spheroids during growth, *J. Cell. Physiol.* 118:53-61 (1984).

[28] J.P. Freyer and P.L. Schor, Regrowth of cells from multicell tumour spheroids, *Cell Tissue Kinet.* 20:249 (1987).

[29] K. Grobe and W. Mueller-Klieser, Distributions of oxygen, nutrient, and metabolic waste concentrations in multicellular spheroids and their dependence on spheroid parameters, *Eur. Biophys. J.* 19:169-181 (1991).

[30] J. Landry, J.P. Freyer and A.M. Sutherland, A model for the growth of multicell spheroids, *Cell Tissue Kinet.* 15:585-594 (1982).

[31] W. Mueller-Klieser, Multicellular spheroids: A review on cellular aggregates in cancer research, *J. Cancer Res. Clin. Oncol.* 113:101-122 (1987).

[32] R.M. Sutherland, J.A. McCredie and W.R. Inch, Growth of multicell spheroids as a model of nodular carcinomas, *J. Nat. Cancer Inst.* 46:113-120 (1971).

[33] R.M. Sutherland and R.E. Durand, Growth and cellular characteristics of multicell spheroids, *Recent Results in Cancer Research* 95:24-49 (1984).

[34] R.M. Sutherland, Cell and environment interactions in tumor microregions: the multicell spheroid model, *Science* 240:177-184 (1988).

[35] E. Wibe, T. Lindmo and O. Kaalhus, Cell kinetic characteristics in different parts of multicellular spheroids of human origin, *Cell Tissue Kinet.* 14:639-651 (1981).

List of Legends for Diagrams

Figure 1(a): Evolution of the tumour radius $R(t)$ in the absence of an inhibitor species($\beta = 0$) and when the proliferation rate is given by $S(\sigma, \beta) = s(\sigma - \tilde{\sigma})$. All initial data converge to the same limiting radius. Parameter values: $\tilde{\sigma} = 0.6, \sigma_B = 1.2, \sigma_R = \Gamma = \lambda = 1.0$. Initial tumour radii: $R(t = 0) = 1, 3, 5$.

Figure 1(b): Evolution of the nutrient concentration σ inside the expanding tumour, showing convergence to a steady configuration, for which cell proliferation ($\sigma > \tilde{\sigma}$) and cell death ($\sigma < \tilde{\sigma}$), averaged over the tumour, are in equilibrium. For comparison, profiles are plotted against the scaled tumour radius $\rho = r/R(t)$ at times $t = 0.00, 0.02, 0.04, ..., 0.20$, and $t = 0.50, 1.00, 1.50, ..., 4.0$. Parameter values are as per figure 1(a) with $R(t = 0) = 3.0$.

Figure 2: Evolution of $R(t)$ when $\beta = 0$ and $S(\sigma, \beta) = s(\sigma - \tilde{\sigma})$, showing decay of the tumour to zero for all initial data. Parameter values: $\tilde{\sigma} = 1.1, \sigma_B = 1.2, \sigma_R = \Gamma = \lambda = 1.0$. Initial tumour radii: $R(t = 0) = 1, 2, 3$.

Figure 3: Evolution of $R(t)$ when $\beta = 0$ and $S(\sigma, \beta) = s\sigma(1 - \sigma/\tilde{\sigma})$ showing decay of the tumour to zero if $R(t = 0) < 7$ and unbounded growth otherwise. Parameter values: $\tilde{\sigma} = 0.6, \sigma_B = 1.2, \sigma_R = \Gamma = \lambda = 1.0$. Initial tumour radii: $R(t = 0) = 4, 6, 8, 10$.

Figure 4: Evolution of $R(t)$ when $\beta = 0$ and $S(\sigma, \beta) = s\sigma(1 - \sigma/\tilde{\sigma})$ showing unbounded growth for all initial data. Parameter values: $\tilde{\sigma} = 1.1, \sigma_B = 1.2, \sigma_R = \Gamma = \lambda = 1.0$. Initial tumour radii: $R(t = 0) = 1, 2, 3$.

Figure 5: Evolution of $R(t)$ when $\beta > 0$ and $S(\sigma, \beta) = s\sigma(1 - \sigma/\tilde{\sigma})(1 - \beta/\tilde{\beta})$ showing decay of the tumour to zero if $R(t = 0) < 0.53$ and convergence to a nonzero configuration otherwise. Parameter values: $\tilde{\sigma} = 0.6, \sigma_B = 1.2, \sigma_R = \Gamma = \lambda = \lambda_1 = 1.0, \tilde{\beta} = 0.95$. Initial tumour radii: $R(t = 0) = 0.25, 0.50, 0.75, 1.00, 2.00, 3.00$.

Figure 6: Evolution of $R(t)$ when $\beta > 0$ and $S(\sigma, \beta) = s\sigma(1 - \sigma/\tilde{\sigma})(1 - \beta/\tilde{\beta})$ showing (slow) convergence to the nonzero steady-state for all initial data. Parameter values: $\tilde{\sigma} = 1.1, \sigma_B = 1.2, \sigma_R = \Gamma = \lambda = \lambda_1 = 1.0, \tilde{\beta} = 0.95$. Initial tumour radii: $R(t = 0) = 0.25, 0.50, 0.75, 1.00$.

Figure 7: Dependence of steady-state tumour radius on the dimensionless parameter grouping Λ, as defined by equations (23) and (24). The existence of nontrivial solutions

is restricted to a finite range of values of Λ.

Figure 8(a): The effect on the scaled steady-state tumour radius $\eta = \sqrt{\lambda} R_S$ of an inhibitor species ($\beta > 0$) is compared with the inhibitor-free situation ($\beta \equiv 0$) as the dimensionless parameter grouping Λ_0 varies. The inhibitor acts both directly, via the cell proliferation rate, and indirectly, consuming the nutrient species. When $\Lambda_1 = 0.5$, the inhibitor-present configurations give rise to smaller steady tumour radii than their inhibitor-free counterparts. Key: inhibitor-present case '——'; inhibitor-free case '- - -'. Parameter values: $\Lambda_1 = 1.0, \Lambda_2 = 0.5, \phi = 1.4, s = 10$.

Figure 8(b): The effect on η of an inhibitor species ($\beta > 0$) is contrasted with the inhibitor-free situation ($\beta \equiv 0$) as the dimensionless parameter grouping Λ_0 varies. When $\Lambda_1 = 1.1$, the existence of nontrivial inhibitor-present solutions is restricted to a smaller range of Λ_0 where they are nonunique, with two nontrivial solutions for each value of Λ_0. Key: inhibitor-present case '——'; inhibitor-free case '- - -'. Parameter values: $\Lambda_1 = 1.0, \Lambda_2 = 1.1, \phi = 1.4, s = 10$.

Figure 8(c): The effect on η of different modes of inhibitor action are compared as the parameter Λ_1 varies. Key: inhibitor-present case (direct action) ' .....'; inhibitor-present case (indirect action) '**.....**'; inhibitor-present case (direct and indirect action) '——'; inhibitor-free case '- - -'. Parameter values: $\Lambda_0 = 0.1, \Lambda_2 = 1.1, \phi = 1.4, s = 10$.

Figure 9: Phase-plane diagram in $(\eta, \frac{d\eta}{dt})$-space showing how the number, and nature, of the critical, or stationary, points vary with the parameter Λ: for $\Lambda > 1/3$, $\eta = 0$ is the unique, stable solution; for $\Lambda \in (0, 1/3)$, the trivial solution is unstable and a nontrivial, stable solution exists. Trajectories are plotted when Λ takes values: (1) $\Lambda = 0.1$; (2) $\Lambda = 0.2$; ...; (5) $\Lambda = 0.5$.

Figure 10: Diagram characterising the domain of existence and stability of nontrivial, time-independent phase I tumours.

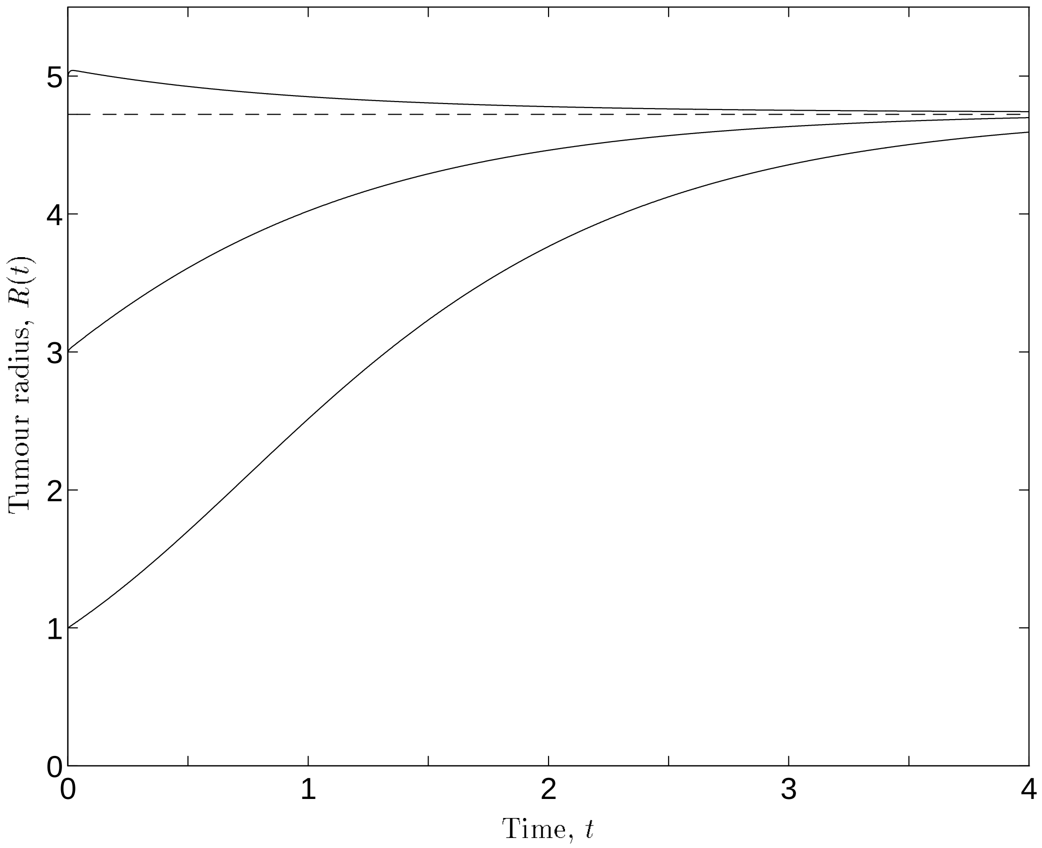

5
4
3
2
1
0
0
1
2
3
4
Tumour radius, $R(t)$
Time, t

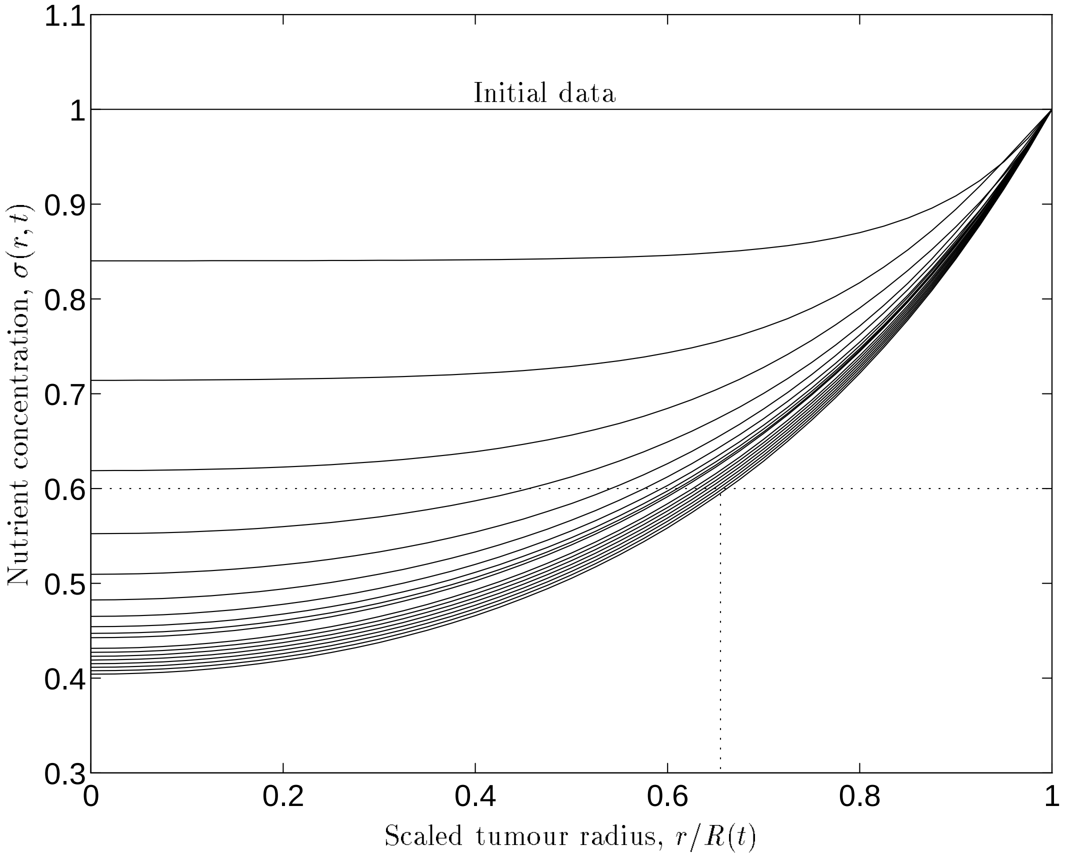
Initial data
Nutrient concentration, $\sigma(r,t)$
Scaled tumour radius, $r/R(t)$
1.1
1
0.9
0.8
0.7
0.6
0.5
0.4
0.3
0
0.2
0.4
0.6
0.8
1

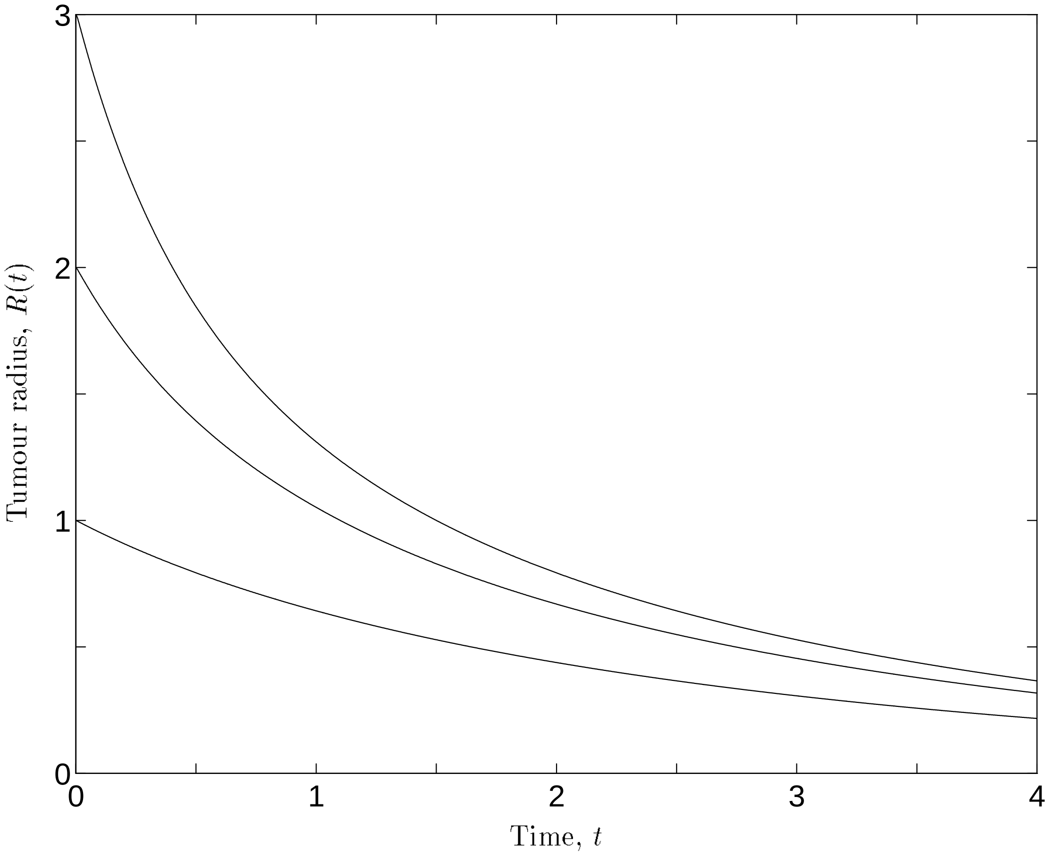
3
2
1
0
0
1
2
3
4
Tumour radius, $R(t)$
Time, t

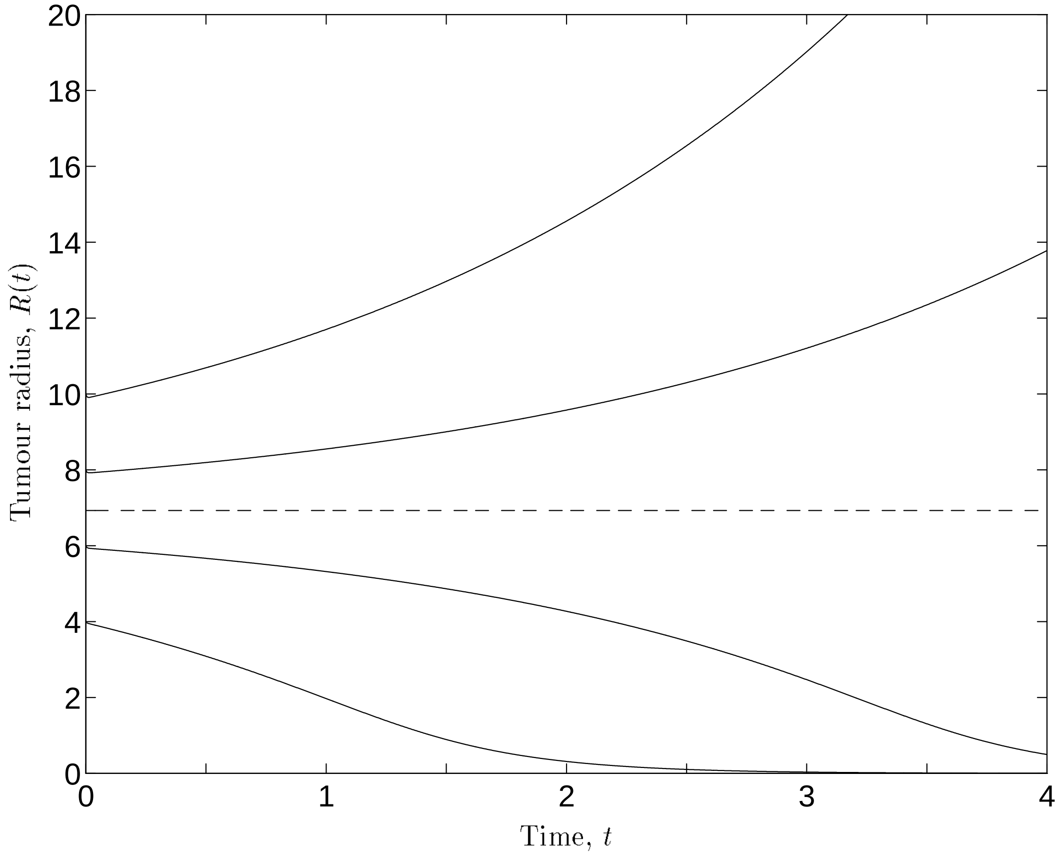

Tumour radius, $R(t)$
0
2
4
6
8
10
12
14
16
18
20
0
1
2
3
4
Time, t

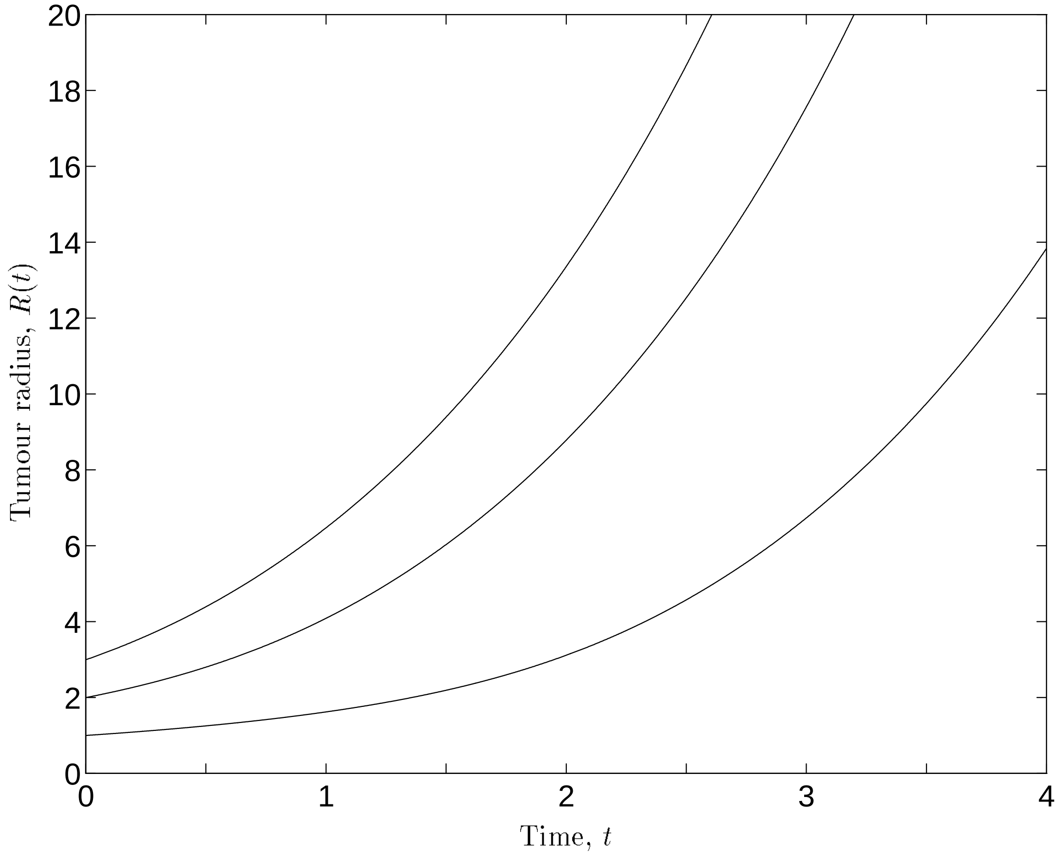
Tumour radius, $R(t)$
Time, t
0
2
4
6
8
10
12
14
16
18
20
0
1
2
3
4

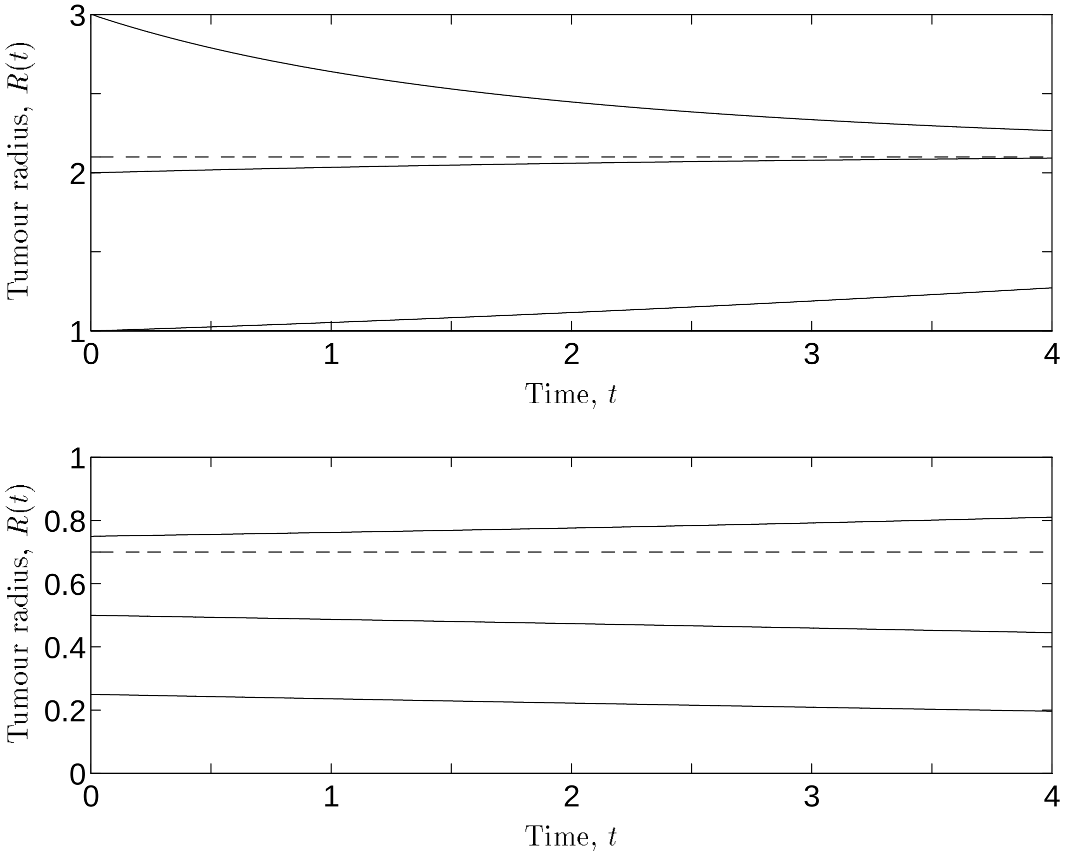

Tumour radius, $R(t)$
3
2
1
0
1
2
3
4
Time, t
Tumour radius, $R(t)$
1
0.8
0.6
0.4
0.2
0
0
1
2
3
4
Time, t

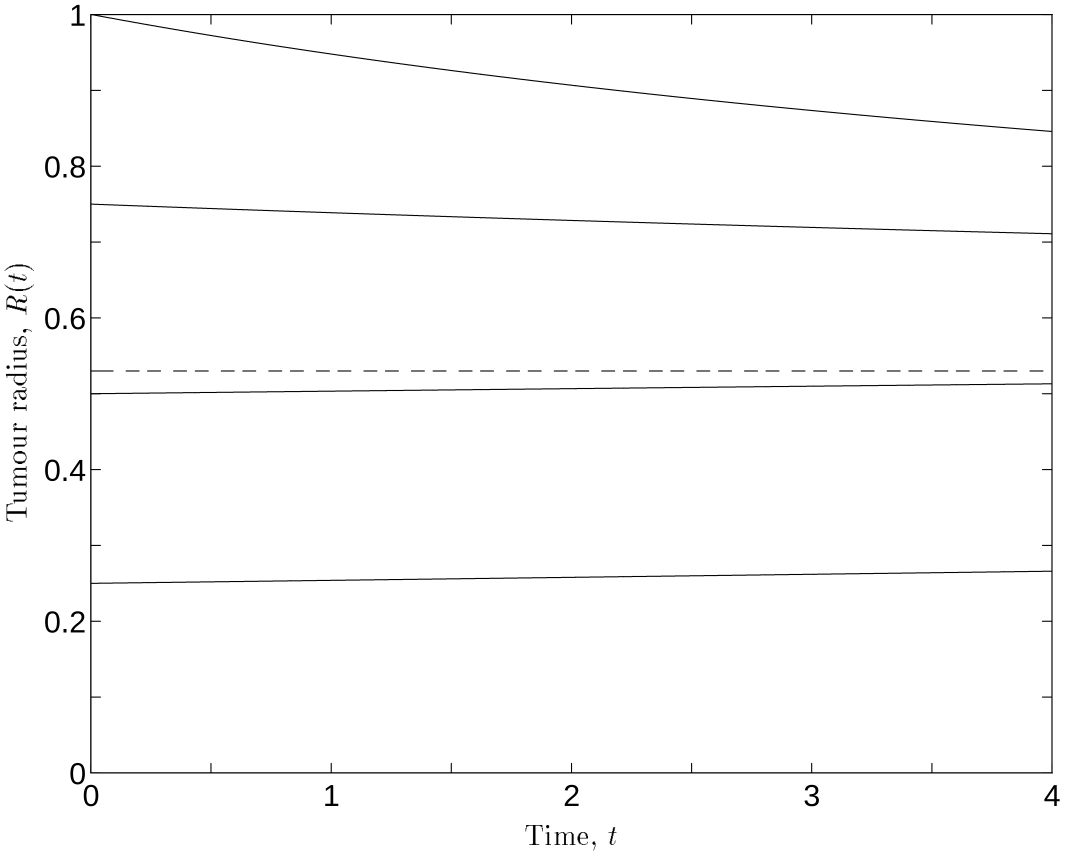

Tumour radius, $R(t)$
Time, t
0
0.2
0.4
0.6
0.8
1
0
1
2
3
4

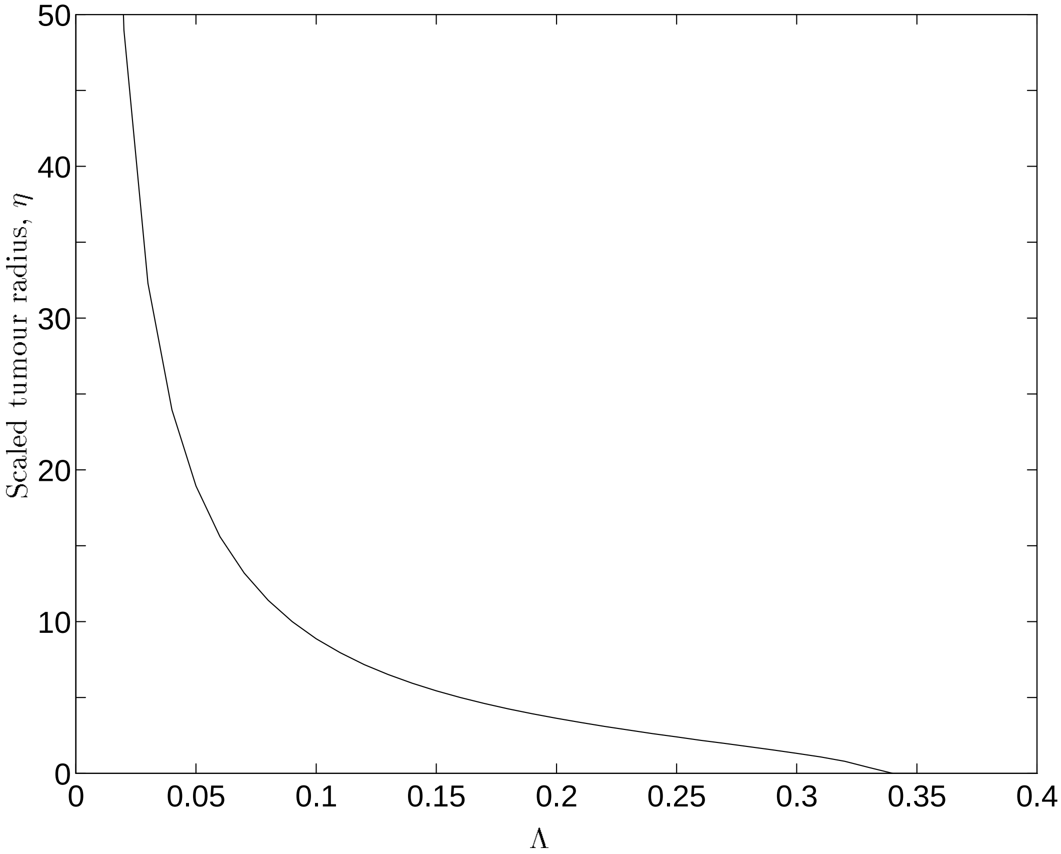

50
40
30
20
10
0
0
0.05
0.1
0.15
0.2
0.25
0.3
0.35
0.4
Scaled tumour radius, η
Λ

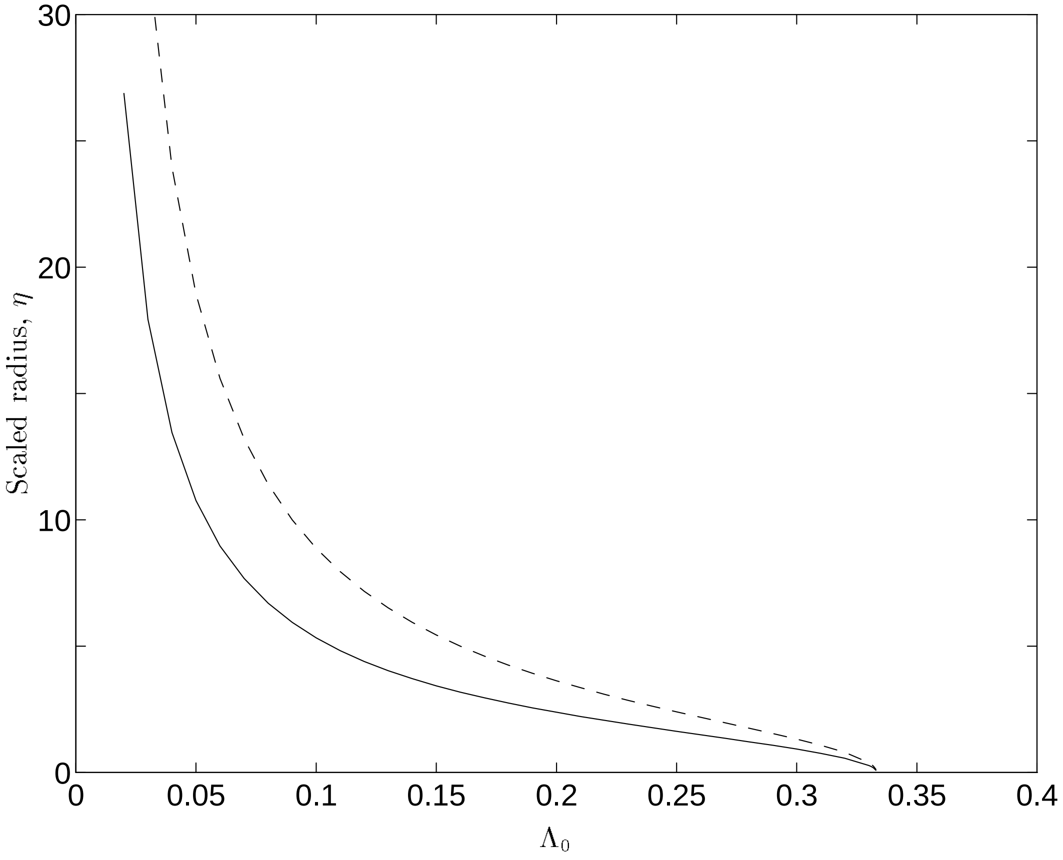

30
20
10
0
0
0.05
0.1
0.15
0.2
0.25
0.3
0.35
0.4
Scaled radius, η
Λ_0

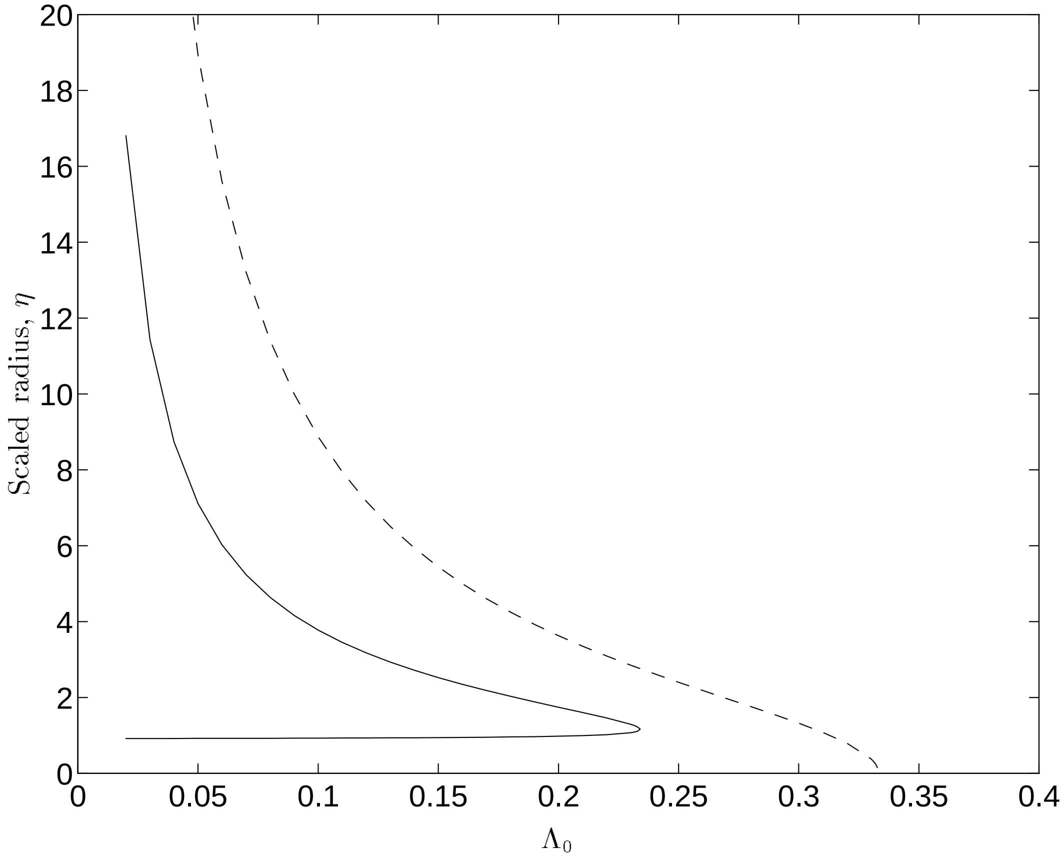
Scaled radius, η
Λ_0
0
2
4
6
8
10
12
14
16
18
20
0
0.05
0.1
0.15
0.2
0.25
0.3
0.35
0.4

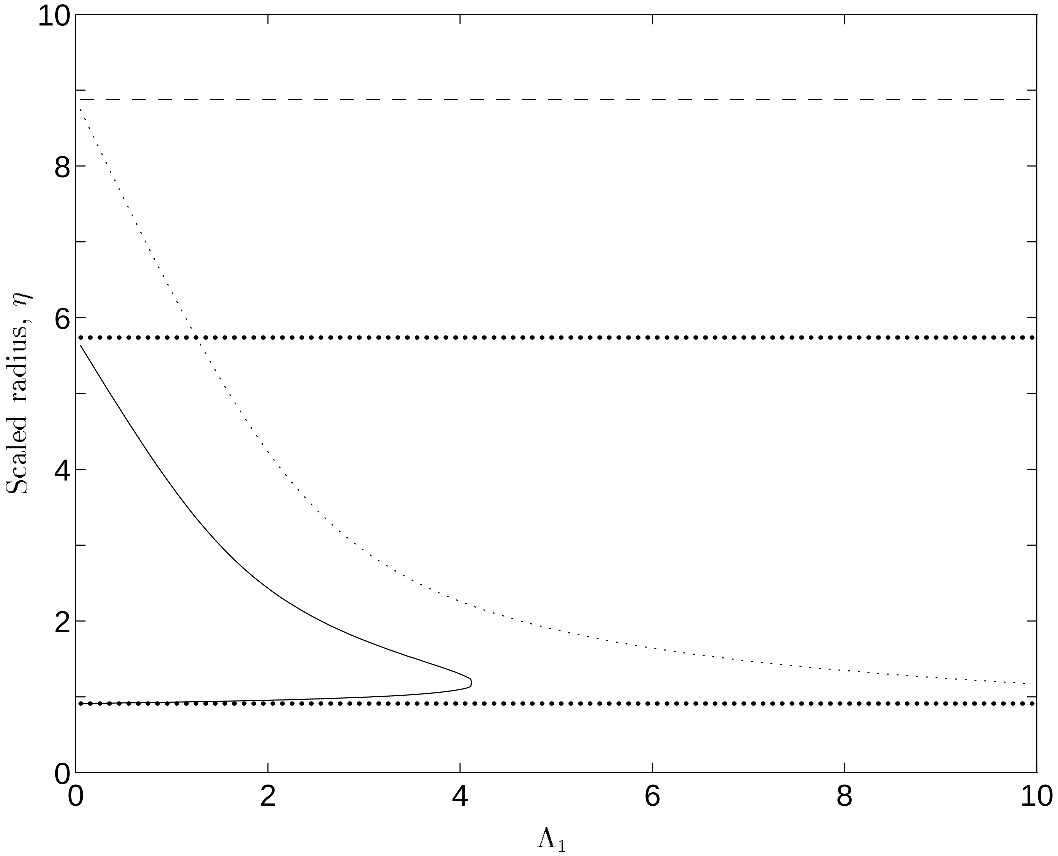
10
8
6
4
2
0
0
2
4
6
8
10
Scaled radius, η
Λ_1

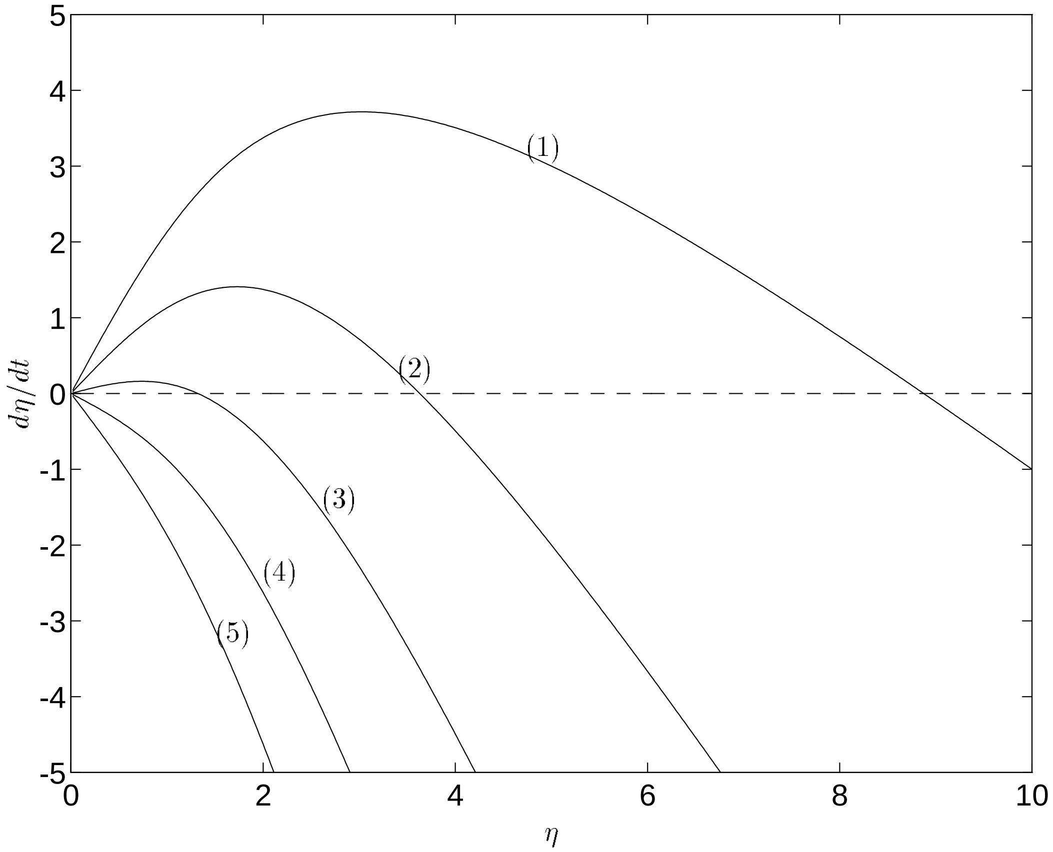

5
4
3
2
1
0
-1
-2
-3
-4
-5
$d\eta/dt$
0
2
4
6
8
10
η
(1)
(2)
(3)
(4)
(5)

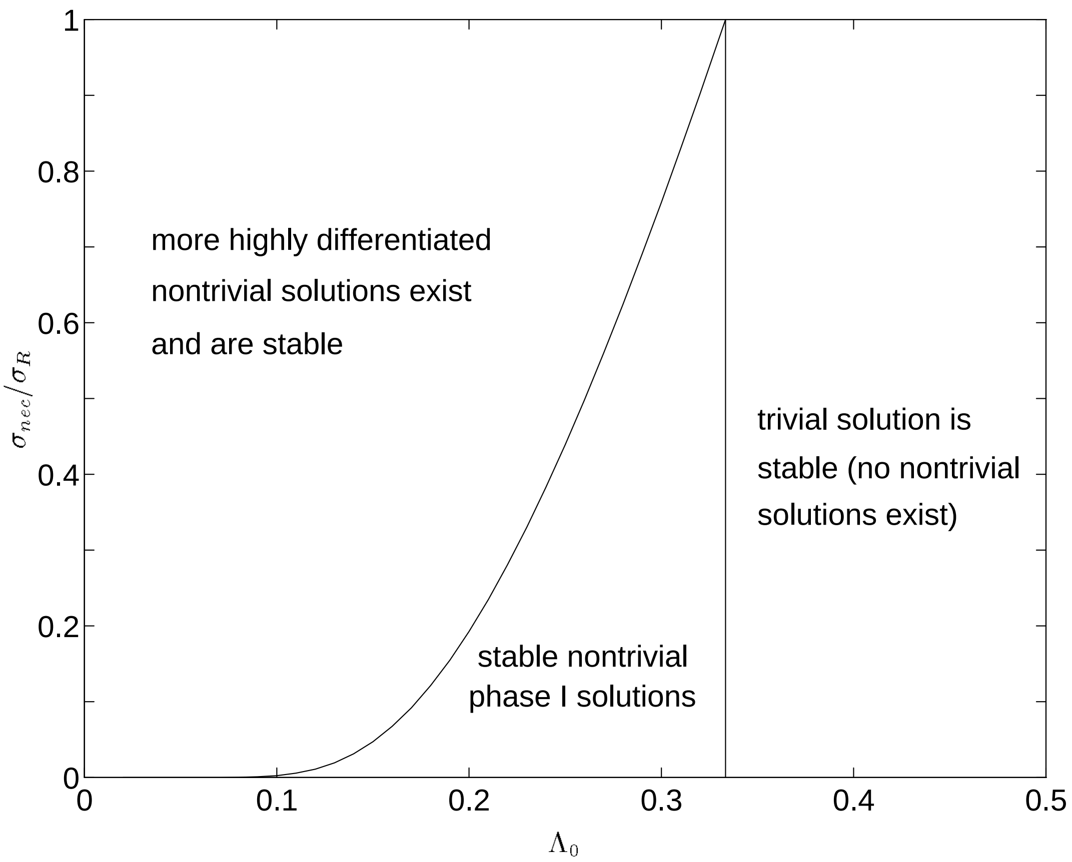
1
0.8
0.6
0.4
0.2
0
0
0.1
0.2
0.3
0.4
0.5
Λ_0
σ_{nec}/σ_R
more highly differentiated
nontrivial solutions exist
and are stable
trivial solution is
stable (no nontrivial
solutions exist)
stable nontrivial
phase I solutions